Folding of Long Chain Alkanediammonium Ions Promoted by a Cucurbituril Derivative – Supporting Information

by *Wei-Hao Huang, Peter Y. Zavalij, and Lyle Isaacs**

Department of Chemistry and Biochemistry, University of Maryland, College Park, MD 20742

Table of Contents **Pages**

Experimental Section.

General. The guests used in this study were purchased from commercial suppliers and were used as their HCl salts. Melting points were measured on a Meltemp apparatus in open capillary tubes and are uncorrected. IR spectra were recorded on Thermo Nicolet IR200 spectrometer and are reported in cm^{-1}. NMR spectra were measured on spectrometers operating at 400, 500, or 600 MHz for ^{1}H and 100 or 125 MHz for ^{13}C. Mass spectrometry was performed using a VG 7070E magnetic sector instrument by fast atom bombardment (FAB) using the indicated matrix or on a JEOL AccuTOF electrospray instrument. Computational results were obtained using Spartan 02 running on a Macintosh personal computer.

Preparation, Purification and Characterization of ns-CB[6]. A mixture of glycoluril (1.42 g, 9.99 mmol), paraformaldehyde (0.50 g, 16.69 mmol), and conc. HCl (4 mL) was heated at 50 ºC for 3 days. The resulting solution was separated by centrifugation and precipated by pouring into MeOH to yield a crude solid (1300 mg). Purification of the mixture was achieved by chromatography on a Dowex 50WX2 column equilibrated with 1:1 formic acid:water. The sample was loaded onto the column as a solution in the eluent (88% HCOOH: (0.2M HCl/H_2O), 1:1, v:v). The fractions of the column were collected and the solvent was removed by rotary evaporation. The resulting solid was washed with MeOH to remove soluble impurities. The CB[6]:*ns*-CB[6] ratio in this crude solid can vary depending on column efficiency. It is possible to decrease the amount of CB[6] by recrystallization from TFA. Final purification of samples containing mainly *ns*-CB[6] can be achieved by suspending in water containing enough hexanediammonium ion to complex the CB[6] impurity. The heterogenous mixture was then

centrifuged and the solid obtained by decanting the supernatant. The solid was washed with several portions of water and dried at high vacuum overnight (47 mg, 3%). M.p. > 300 ºC. IR (KBr, cm^{-1}): 3271w, 1726s, 1466s, 1414s, 1375s, 1326s, 1149s, 964s, 667s, 617s, 796s. ^{1}H NMR (400 MHz, 35% DCl): 5.69 (d, *J* = 8.8, 2H), 5.64 (d, *J* = 8.8, 2H), 5.55-5.35 (m, 18H), 5.17 (d, *J* = 16.0, 1H), 4.44 (d, *J* = 16.0, 1H), 4.40-4.20 (m, 10H). ^{13}C NMR (100 MHz, 35% DCl, ext. dioxane reference): 159.3, 159.0, 155.9, 155.8, 155.6, 73.2, 69.9, 69.8, 69.7, 69.6, 67.6, 53.6, 51.3, 51.2, 50.9, 50.7. (only 16 of the 19 expected resonances were observed). MS (ES): *m/z* 562 (100, $[M + p\text{-xylenediamine} + 2H]^{2+}$, *m/z* spacing = 0.5 confirmed for molecular ion).

Compound **2**. Compound **1** (100 mg, 0.10 mmol) was dissolved in HCl (0.2 mL) and *o*-phthaldialdehyde (13.4 mg, 0.10 mmol) was added to the mixture. The reaction mixture was stirred at room temperature for two days. The reaction mixture was poured into MeOH (5 mL), the solid isolated by filtration, and dried overnight at high vacuum. The crude solid (80 mg), was recrystallized from TFA (2.6 mL) to yield **2** (64 mg, 57%) as a white solid. IR (neat, cm^{-1}): 3474w, 3014s, 2926s, 1726s, 1463s, 1416s, 1376s, 1326s, 1293s, 1225s, 1175s, 962s, 795s, 755s, 671s, 628s. ^{1}H NMR (400 MHz, D_2O): 7.35 (br, 2H), 7.29 (br, 2H), 6.70 (s, 2H), 5.65-5.35 (m, 22H), 4.25-4.00 (d, 10H), 2.34 (d, *J* = 12.0, 1H). ^{13}C NMR (125 MHz, D_2O): 163.4, 160.6, 157.8, 157.0, 135.3, 131.0, 125.4, 118.2, 115.9, 85.0, 71.5, 71.4, 71.2, 71.0, 69.7, 53.1, 52.7, 52.2, 51.8. (not all of the 23 expected resonances were observed). ES-MS: *m/z* 1101 (100, $[M + H]^{+}$: ($[M + H]^{+}$, $C_{43}H_{40}N_{24}$, calcd 1100.32). X-ray crystal structure (from TFA).

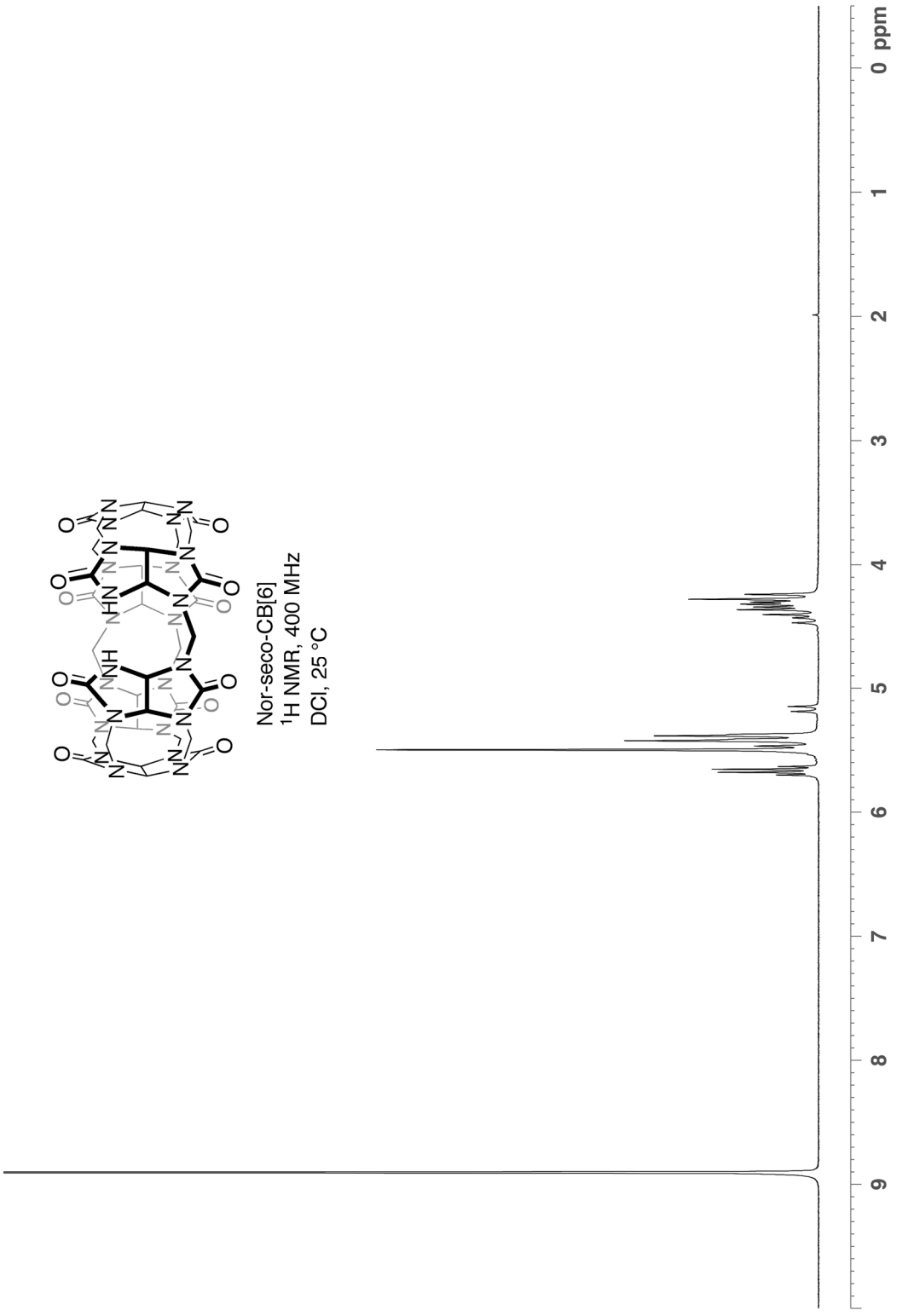

Figure S1. ^{1}H NMR spectrum recorded for *ns*-CB[6] (400 MHz, 35% DCl, 25 ºC).

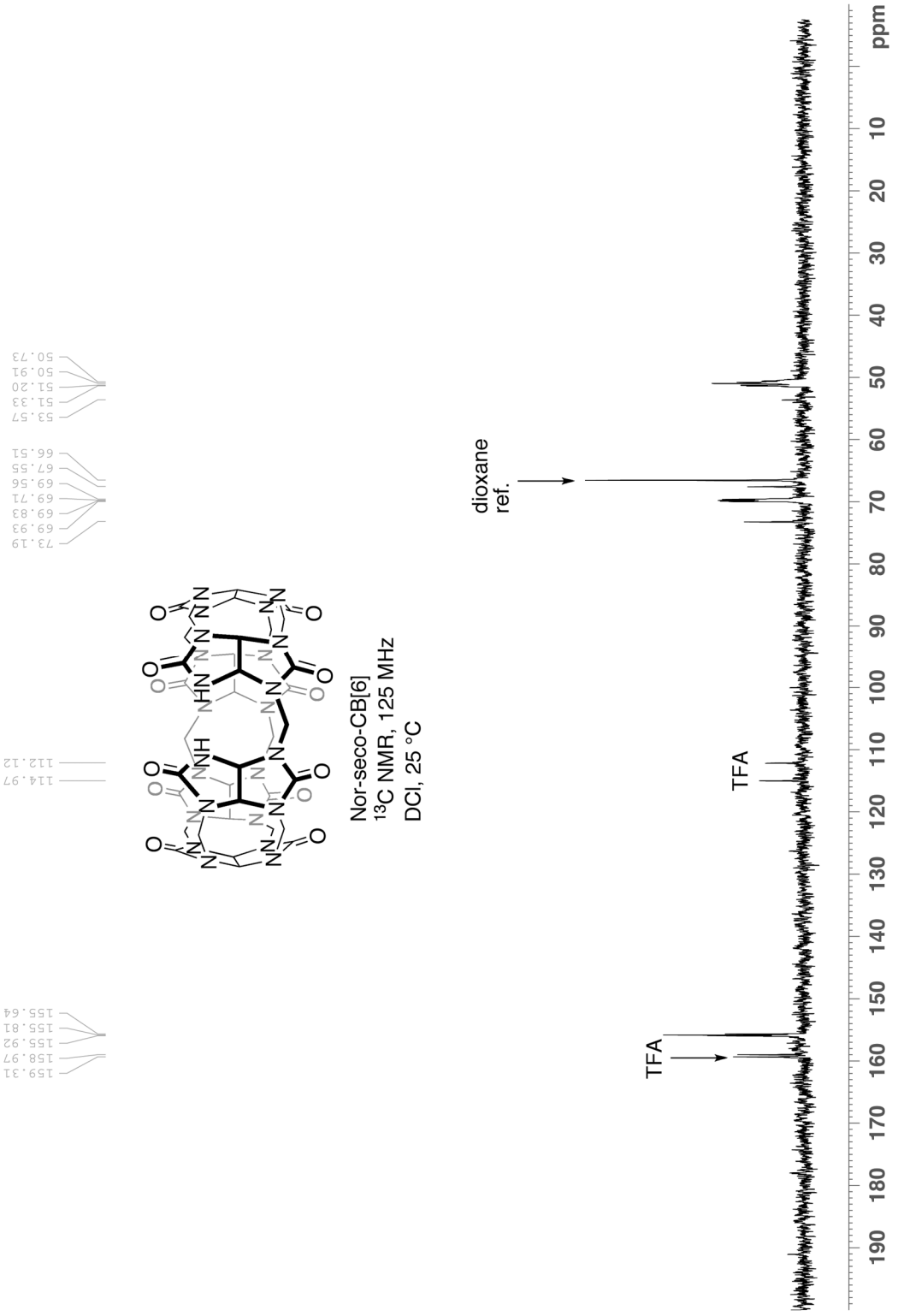

Figure S2. ^{13}C NMR spectrum recorded for *ns*-CB[6] (125 MHz, 35% DCl, 25 ºC).

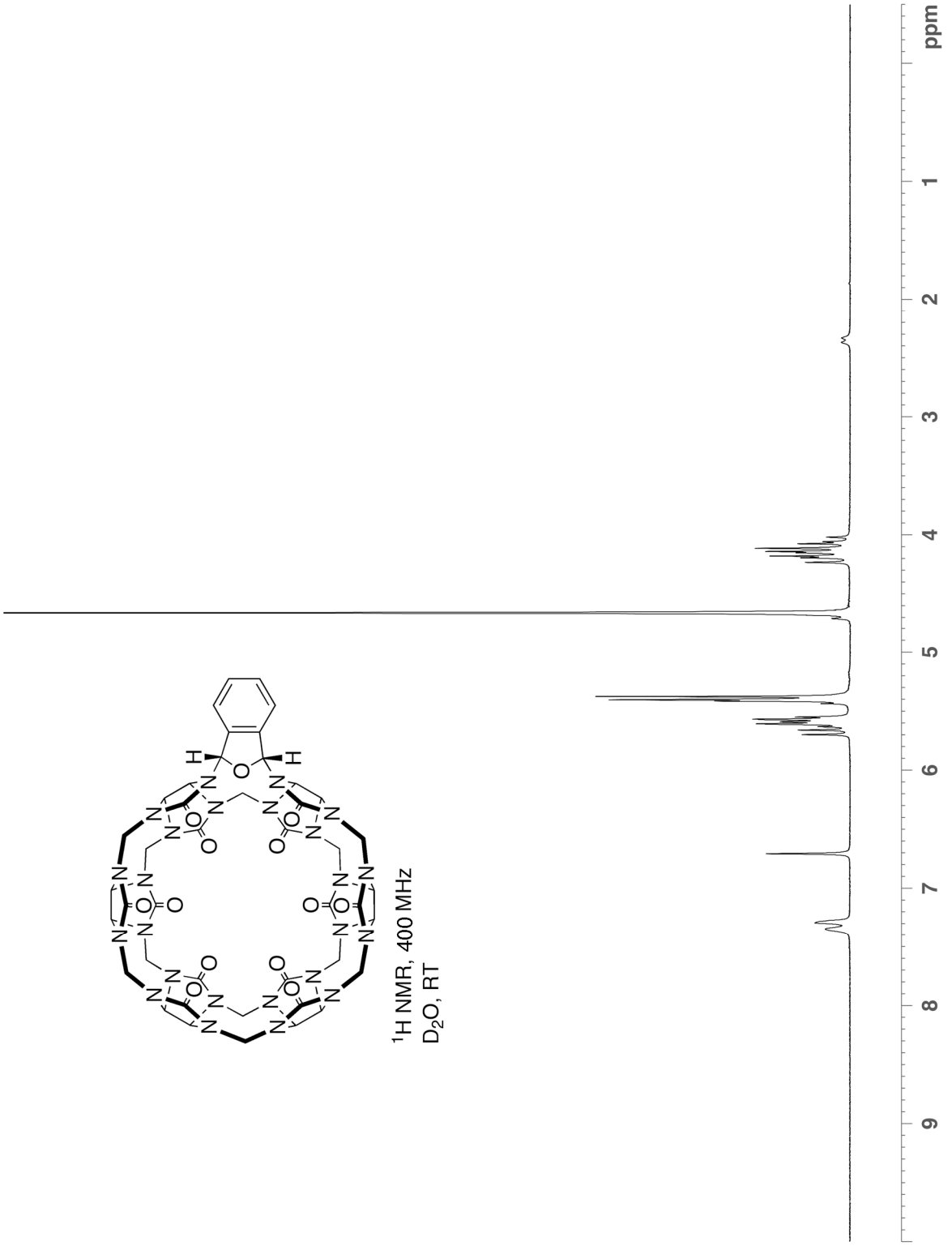

Figure S3. ^{1}H NMR spectrum recorded for **2** (400 MHz, D_2O, 25 ºC).

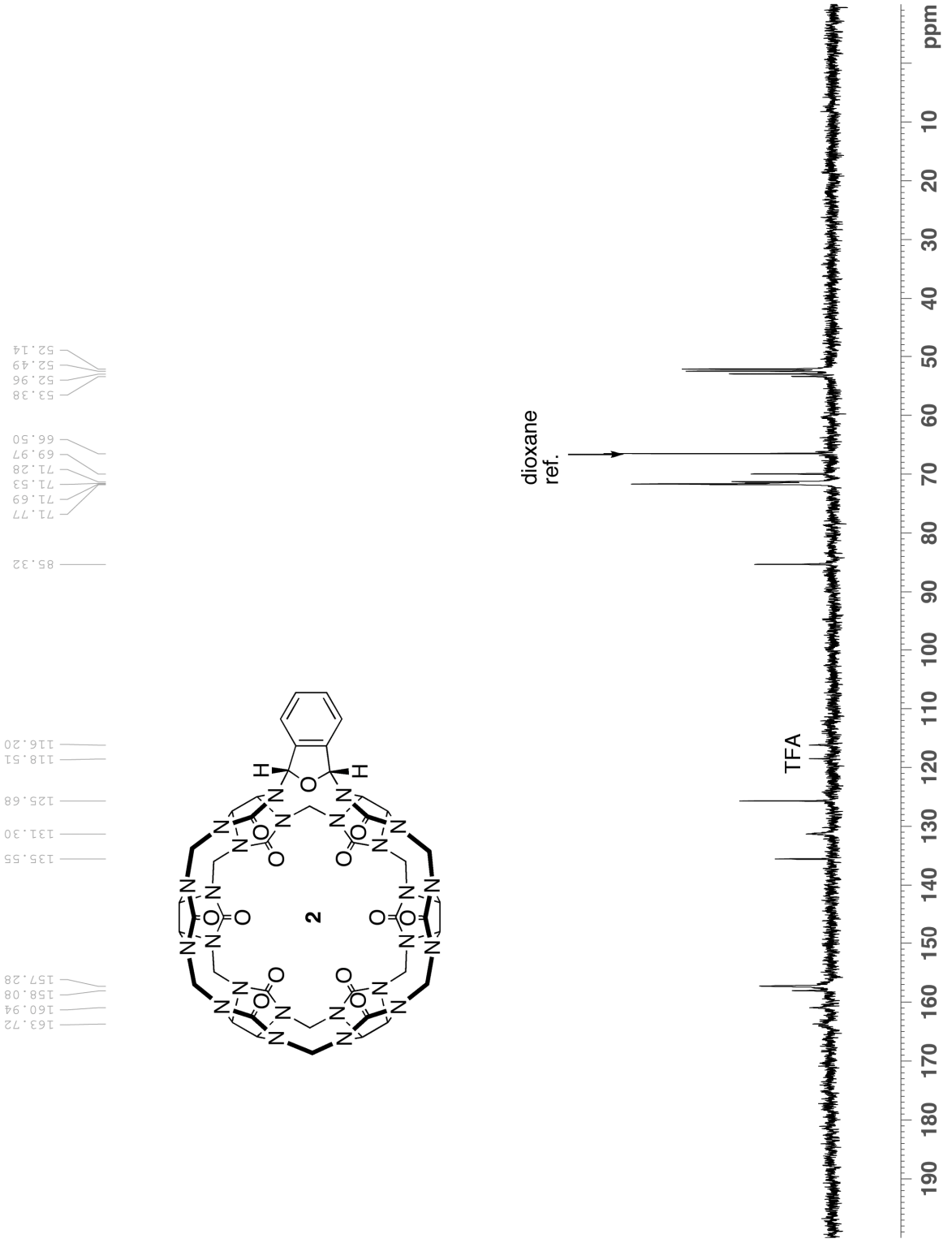

Figure S4. ^{13}C NMR spectrum recorded for **2** (125 MHz, D_2O, 25 ºC).

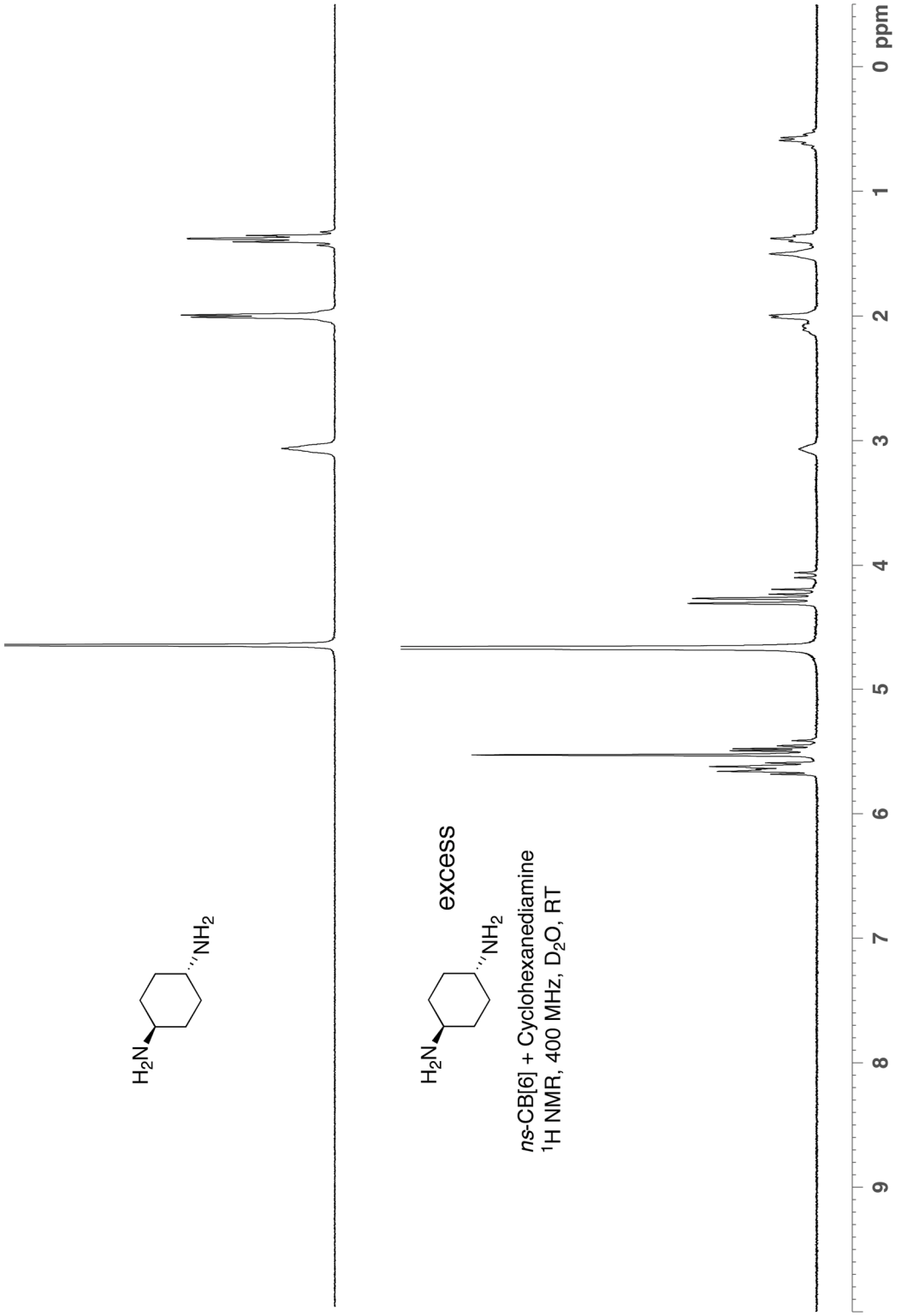

Figure S5. ^{1}H NMR spectra recorded for cyclohexanediamine and its complex with *ns*-CB[6] (400 MHz, D_2O, 25 ºC).

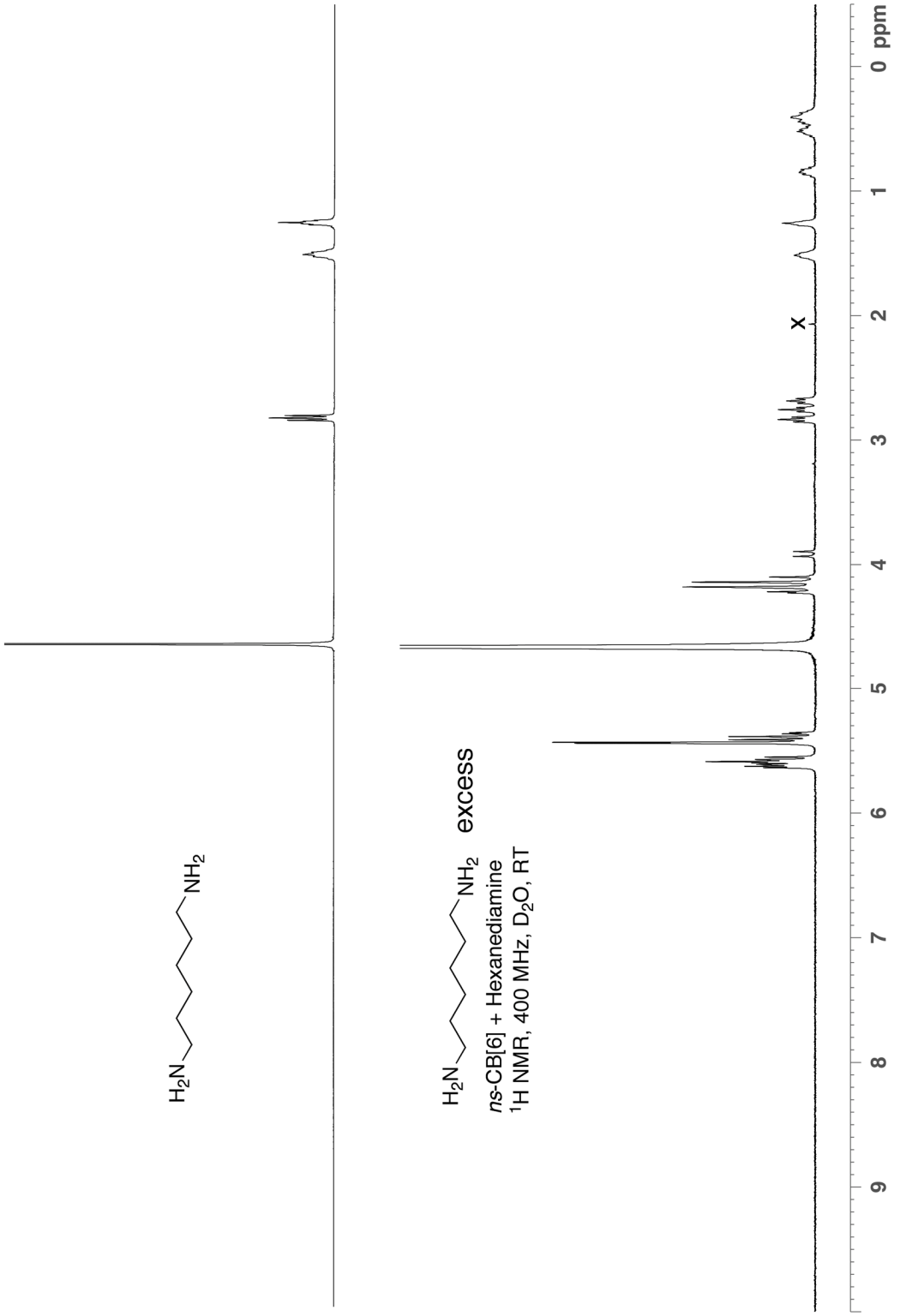

Figure S6. ^{1}H NMR spectra recorded for hexanediamine and its complex with *ns*-CB[6] (400 MHz, D_2O, RT, x = trace acetone impurity).

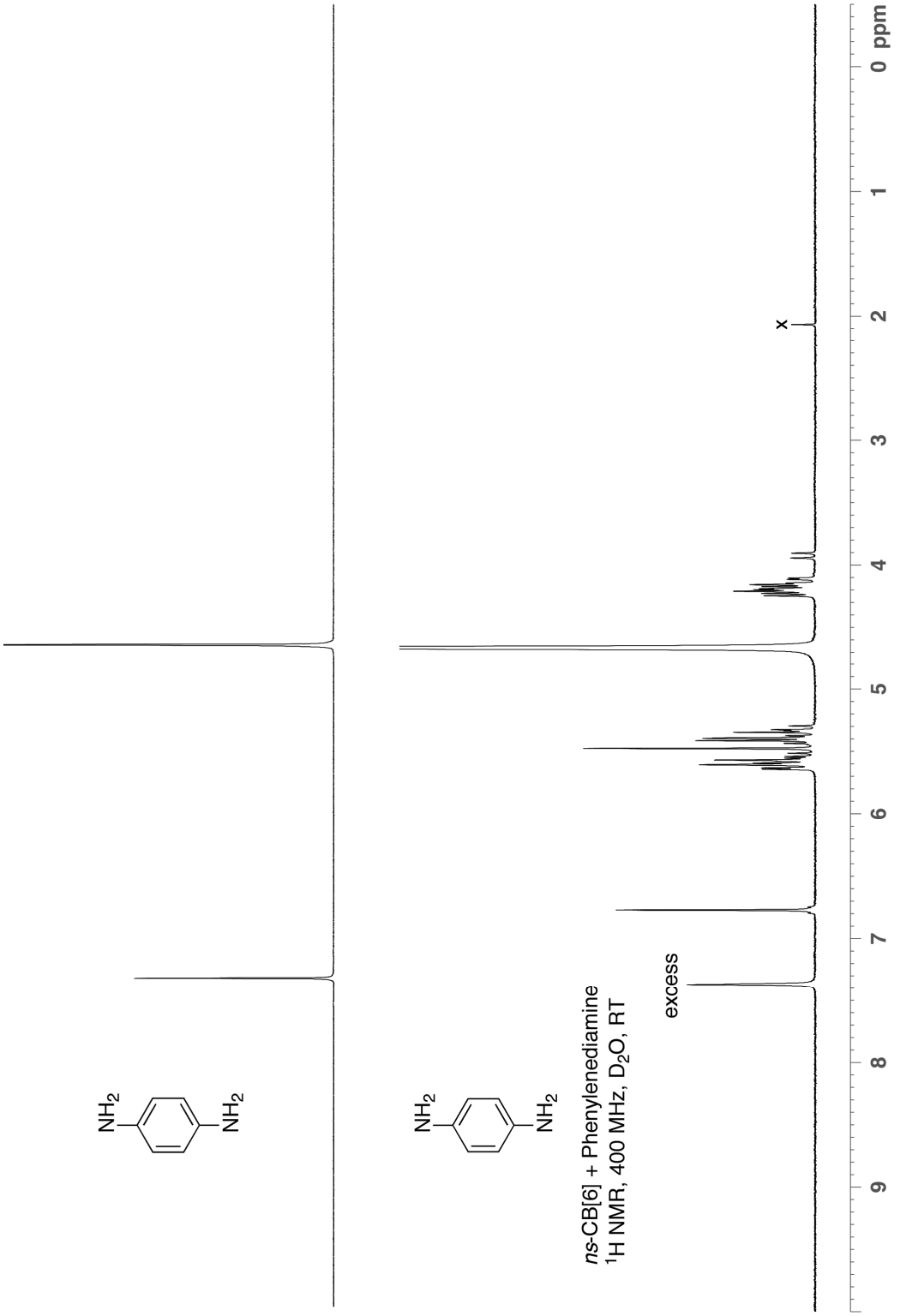

Figure S7. ^{1}H NMR spectra recorded for phenylenediamine and its complex with *ns*-CB[6] (400 MHz, D_2O, RT, x = trace acetone impurity).

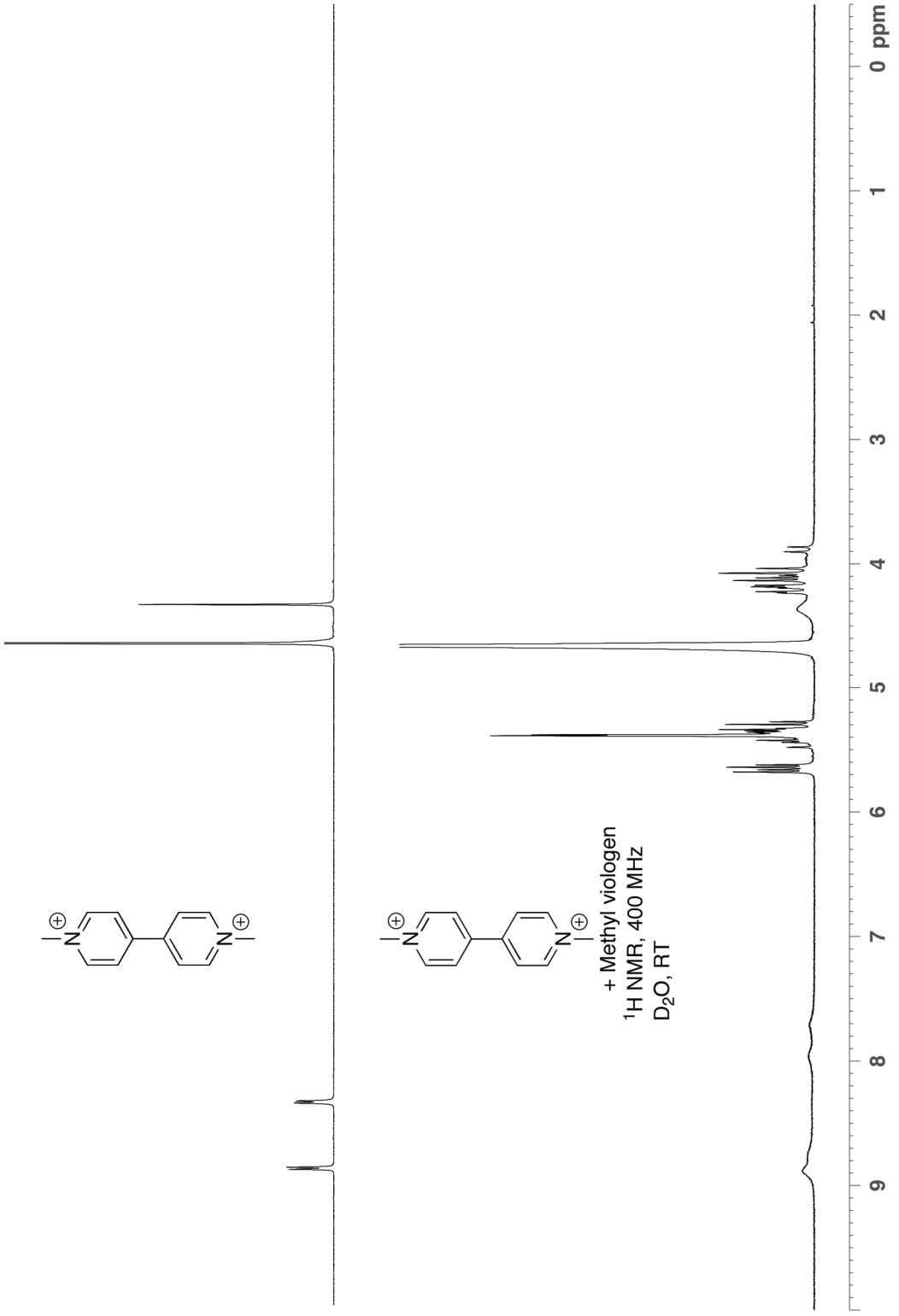

Figure S8. ^{1}H NMR spectra recorded for methyl viologen and its complex with *ns*-CB[6] (400 MHz, D_2O, RT).

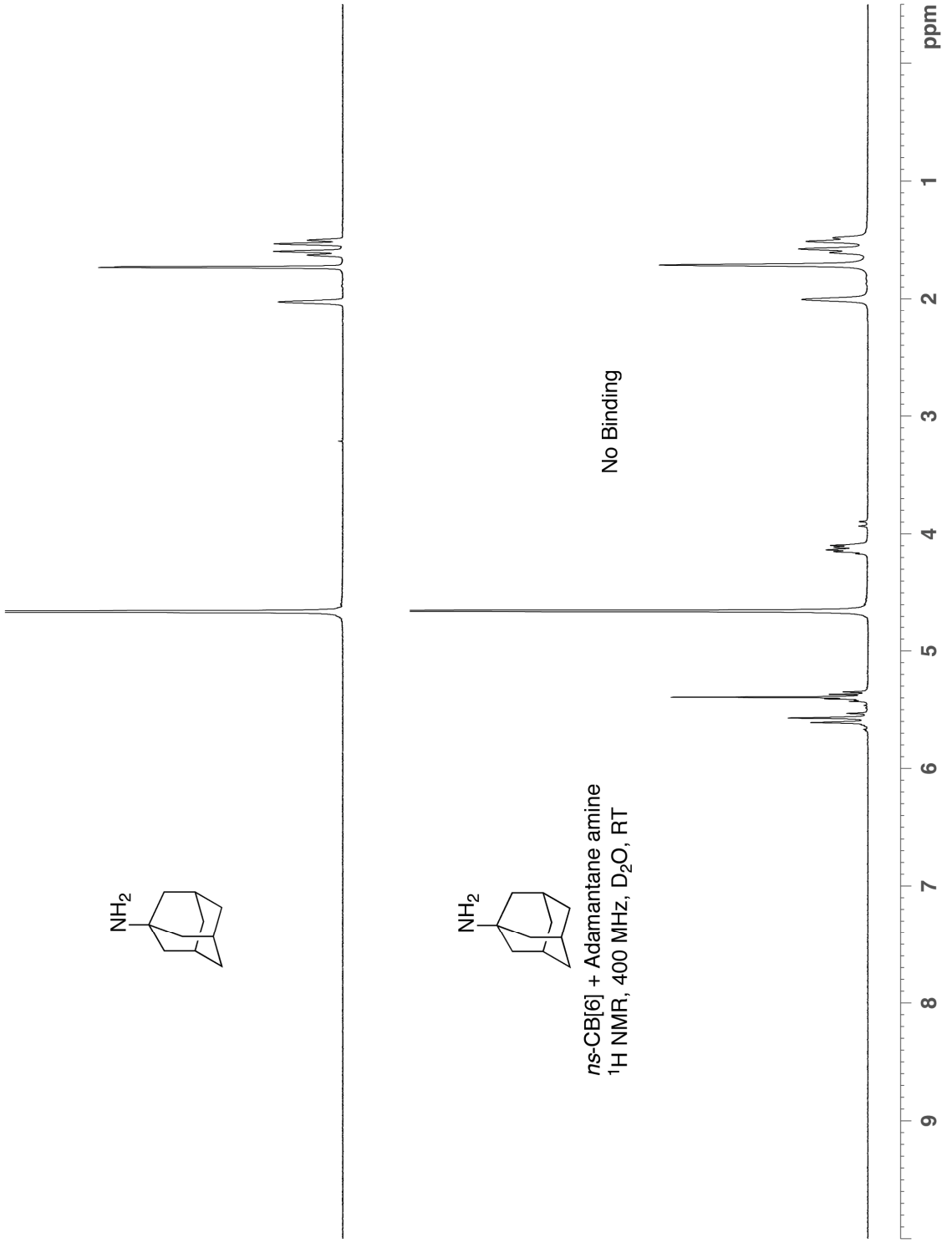

Figure S9. ^{1}H NMR spectra recorded for 1-aminoadamantane and its non-binding mixture with *ns*-CB[6] (400 MHz, D_2O, RT).

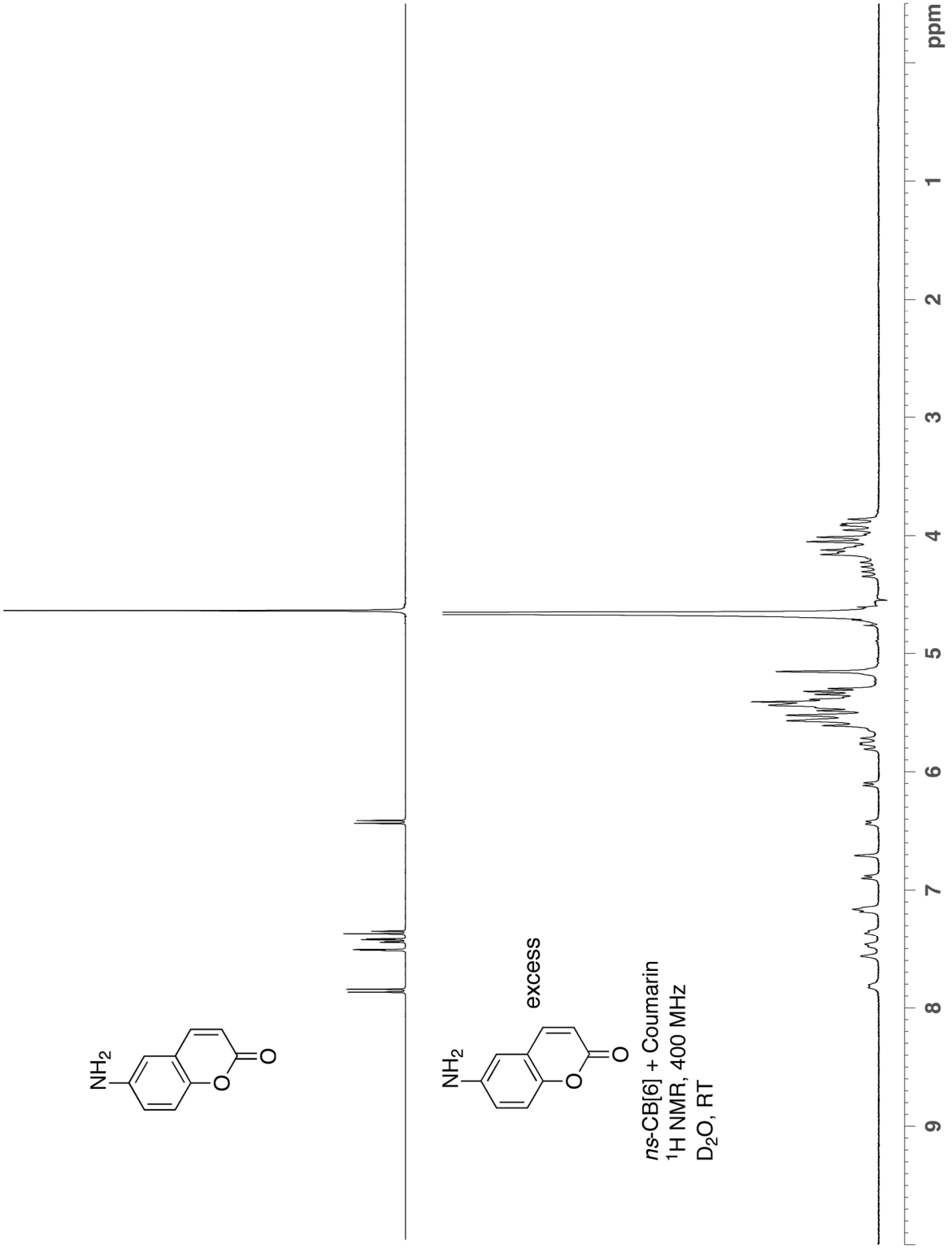

Figure S10. ^{1}H NMR spectra recorded for aminocoumarin and its complex with *ns*-CB[6] (400 MHz, D_2O, RT).

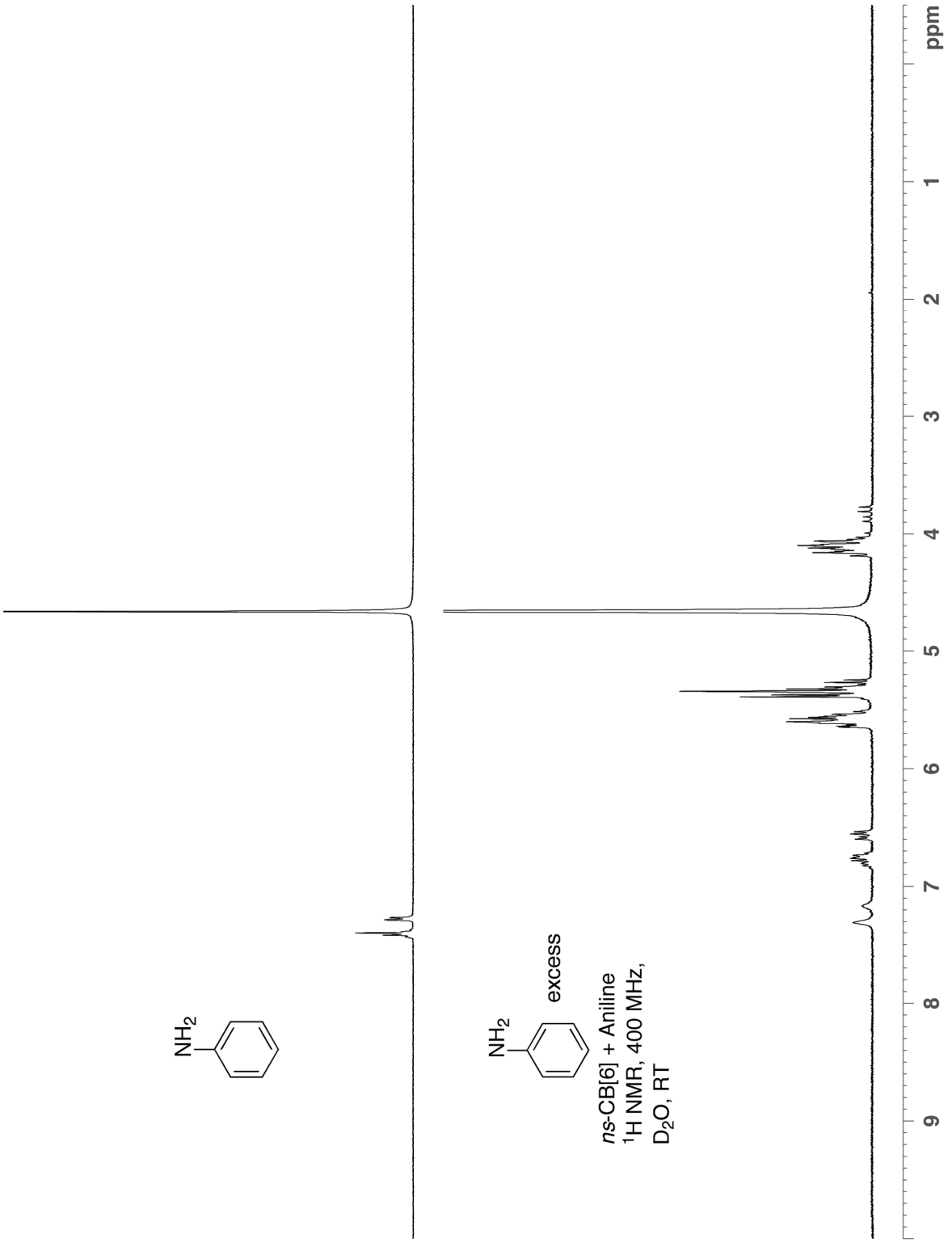

Figure S11. ^{1}H NMR spectra recorded for aniline and its complex with *ns*-CB[6] (400 MHz, D_2O, RT). The ratio of the two diastereomers is 67:33.

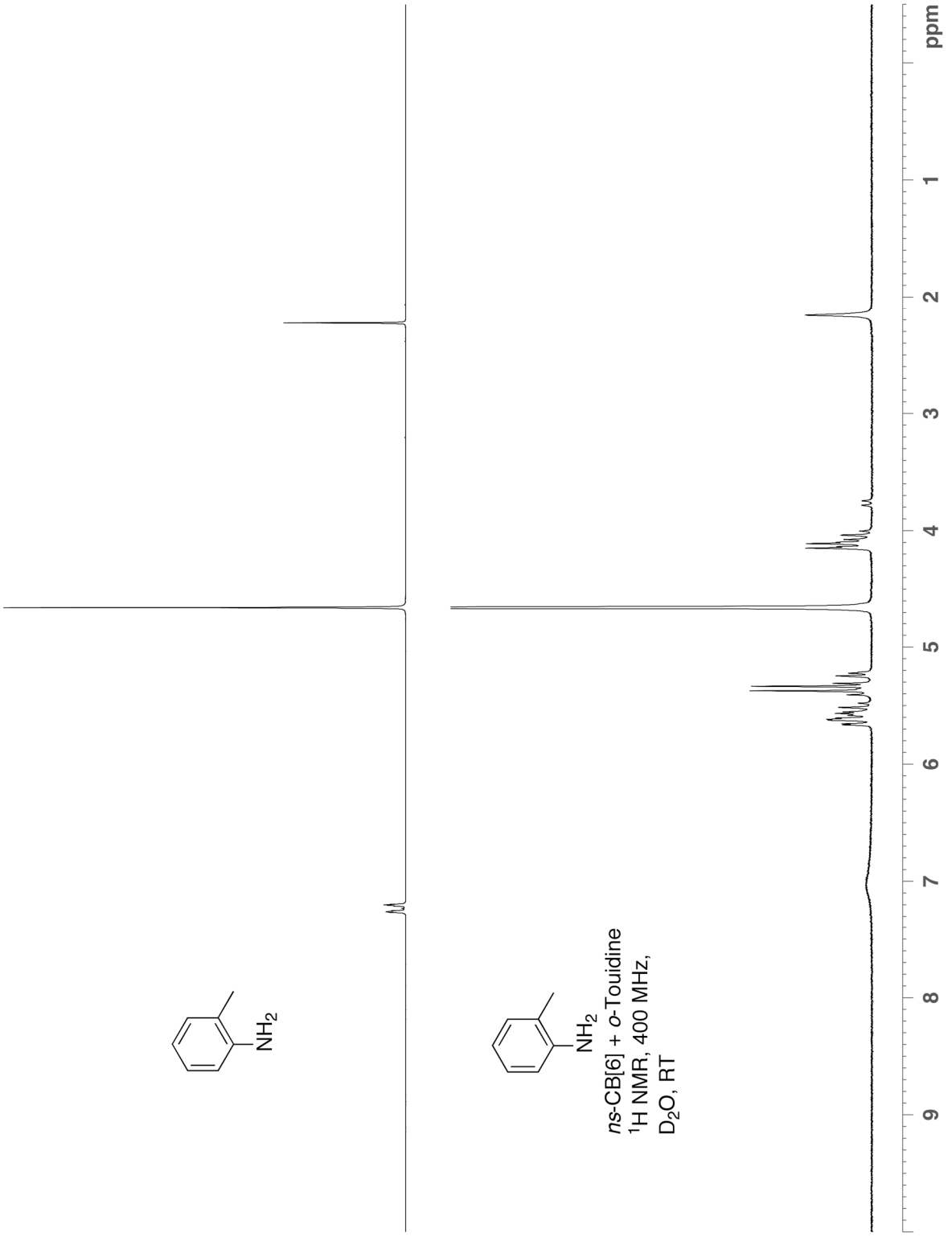

Figure S12. ^{1}H NMR spectra for *o*-toluidine and its mixture with *ns*-CB[6] (400 MHz, D_2O, RT).

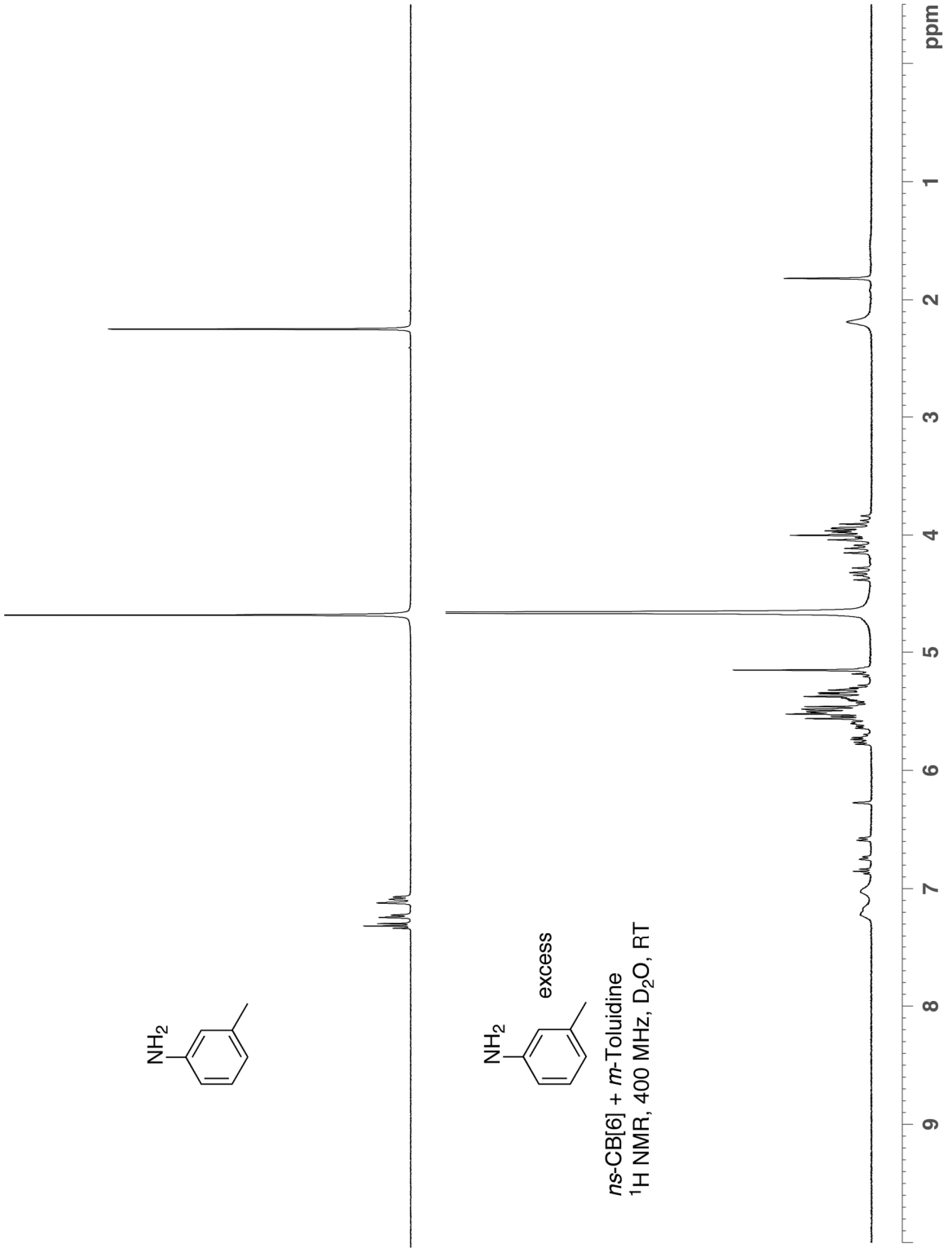

Figure S13. ^{1}H NMR spectra recorded for *m*-toluidine and its complex with *ns*-CB[6] (400 MHz, D_2O, RT).

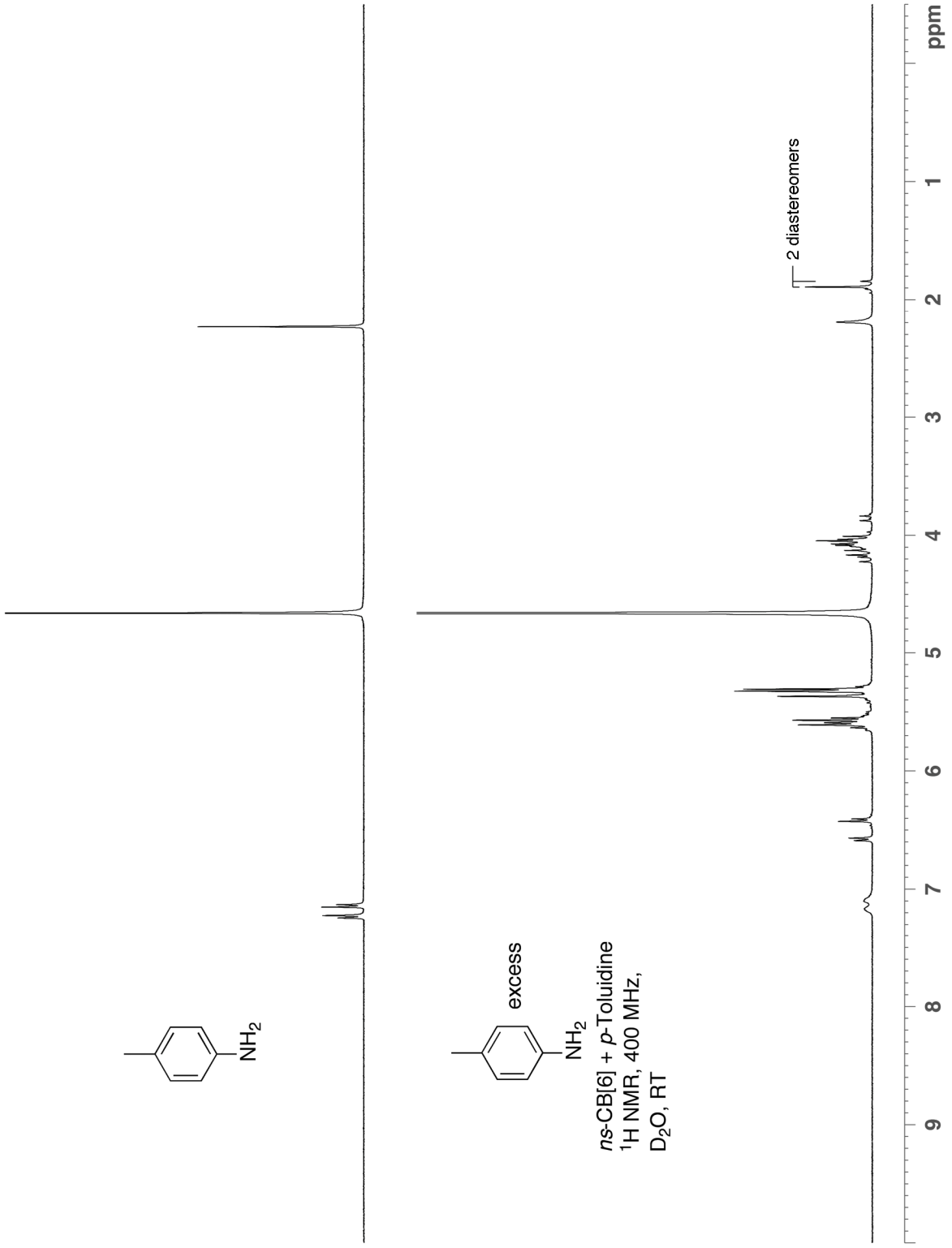

Figure S14. ^{1}H NMR spectra recorded for *p*-toluidine and its complex with *ns*-CB[6] (400 MHz, D_2O, RT). The ratio of the two diastereomers is 76:24.

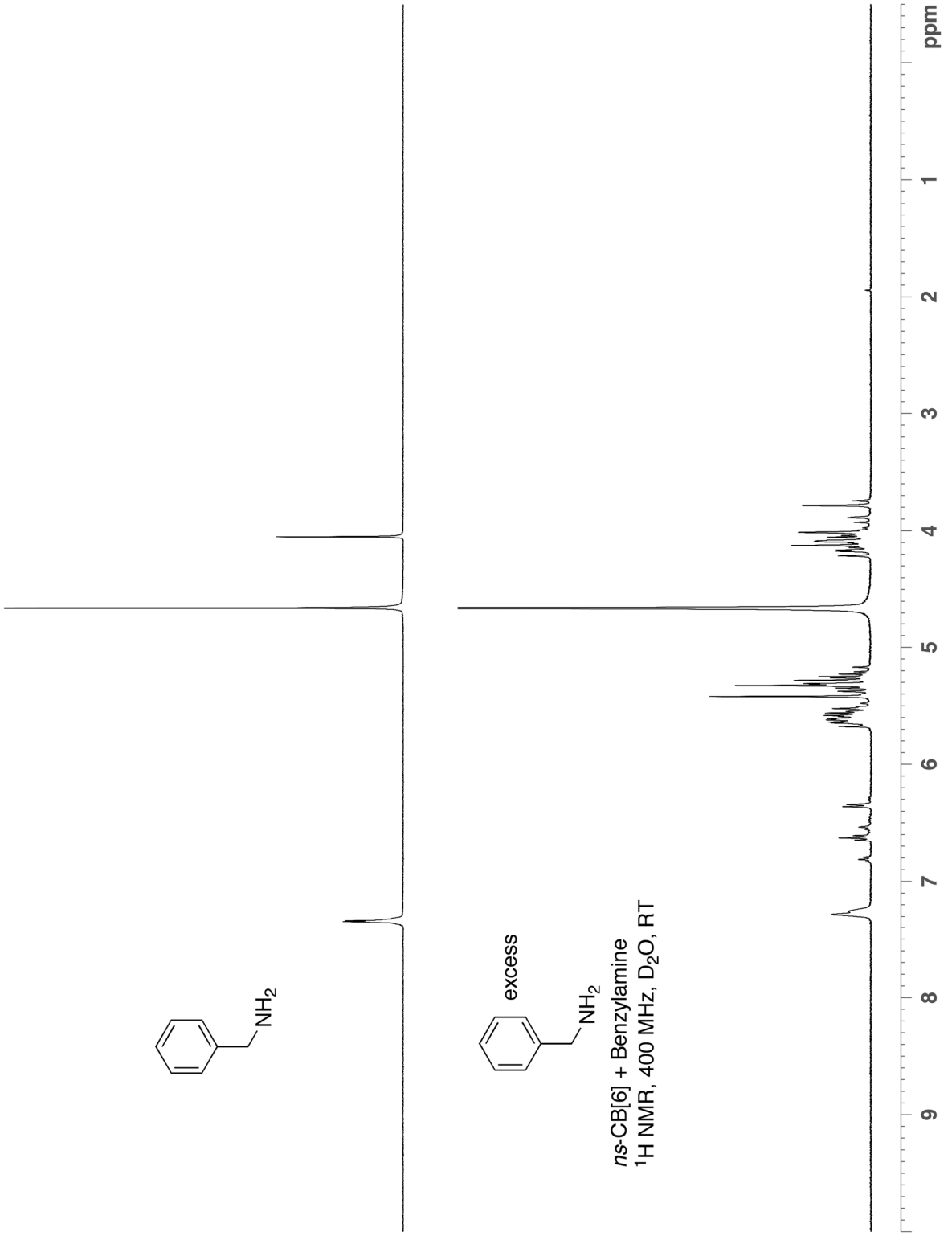

Figure S15. ^{1}H NMR spectra recorded for benzylamine and its complex with *ns*-CB[6] (400 MHz, D_2O, RT).

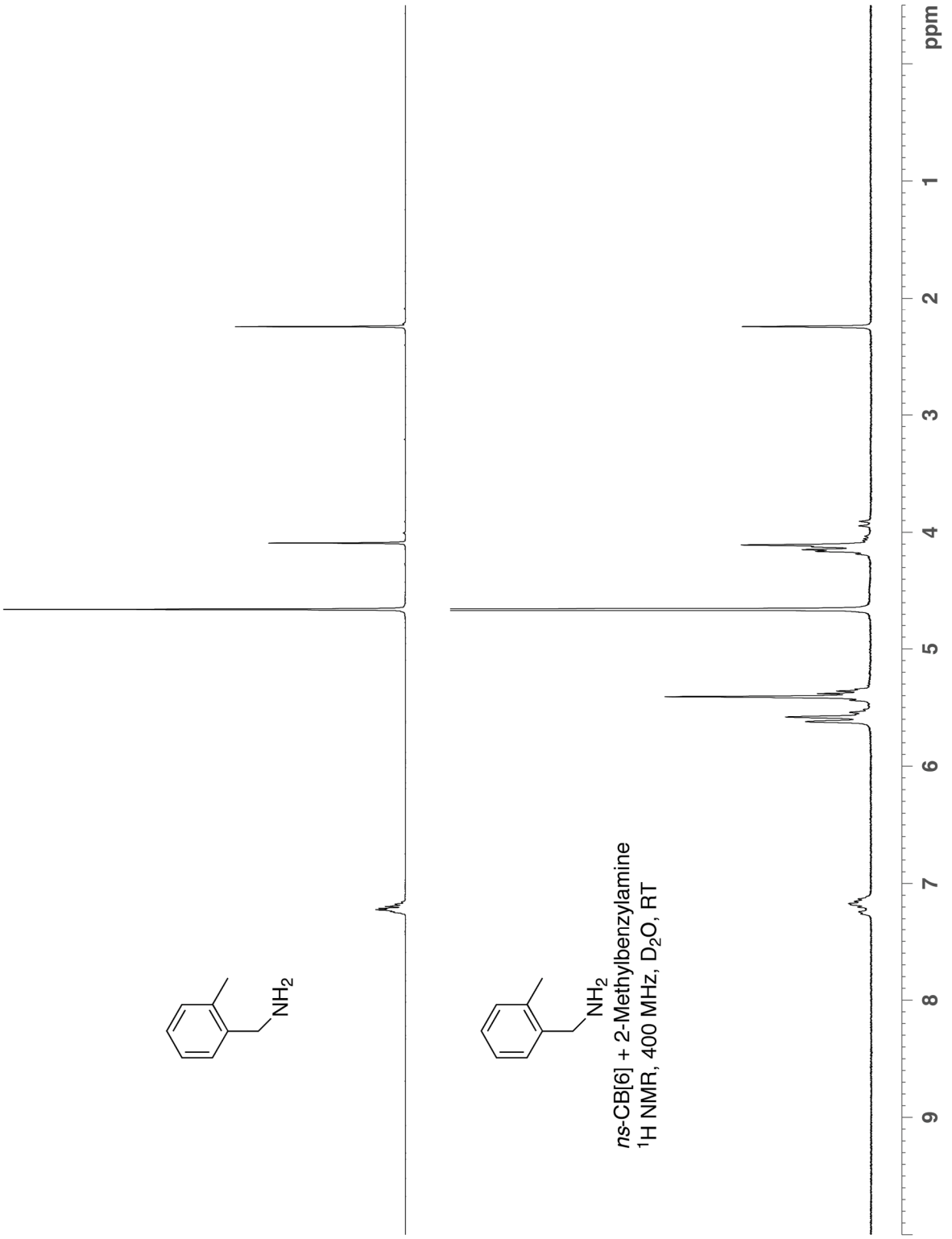

Figure S16. ^{1}H NMR spectrum recorded for 2-methylbenzylamine and when mixed with *ns*-CB[6] (400 MHz, D_2O, RT).

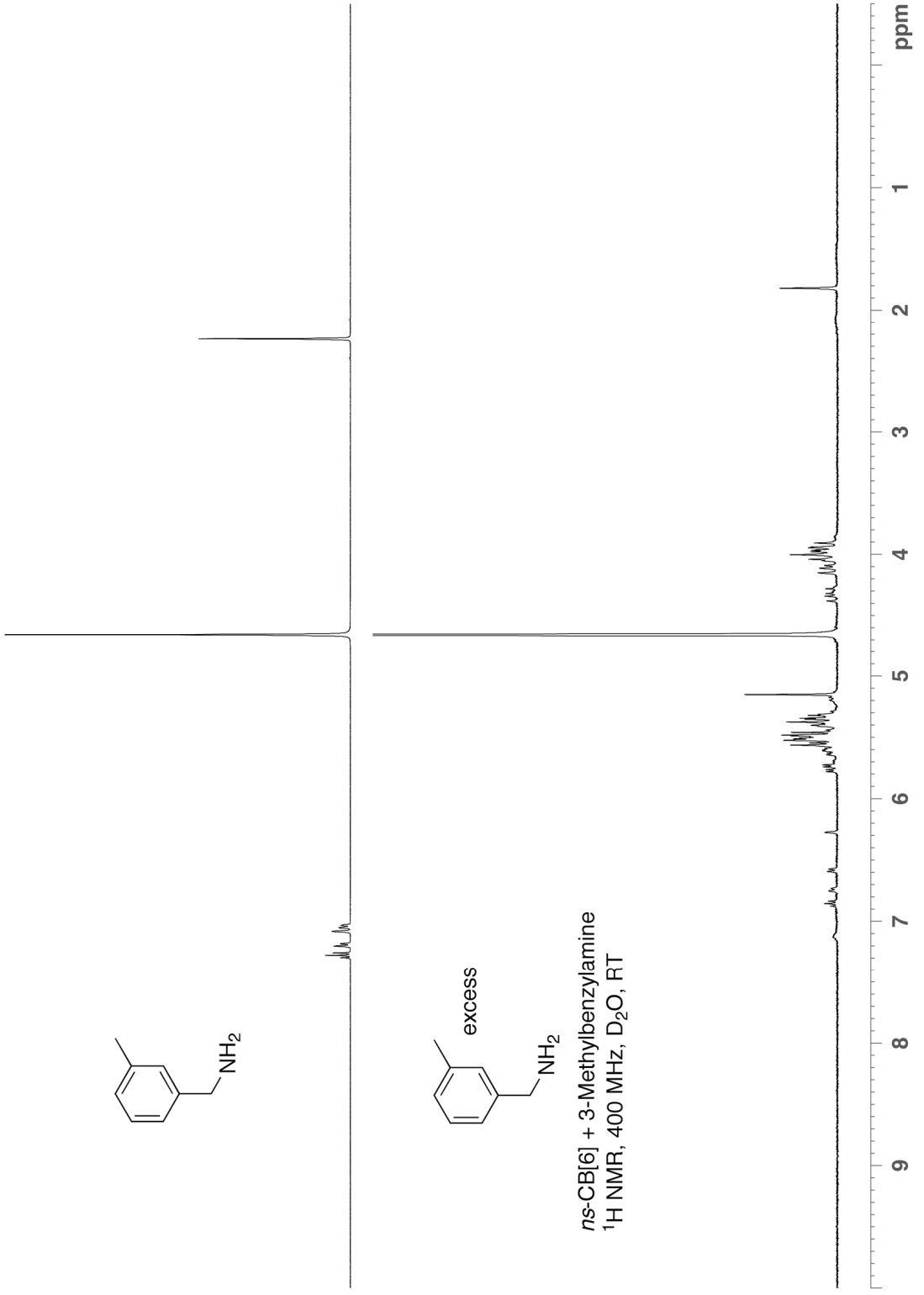

Figure S17. ^{1}H NMR spectra recorded for 3-methylbenzylamine and its complex with *ns*-CB[6] (400 MHz, D_2O, RT).

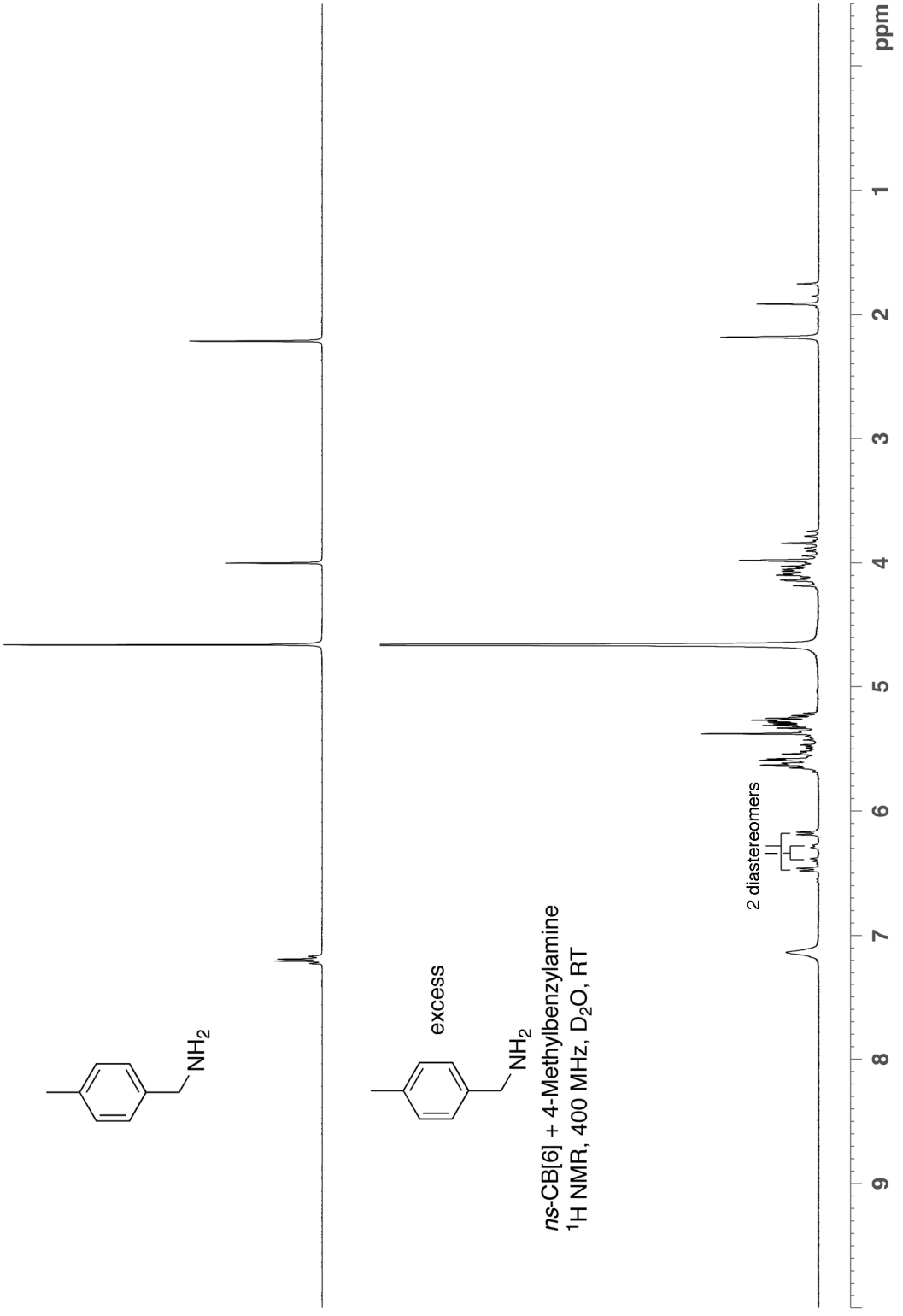

Figure S18. ^{1}H NMR spectra recorded for 4-methylbenzylamine and its complex with *ns*-CB[6] (400 MHz, D_2O, RT). The ratio of the two diastereomers is 71:29.

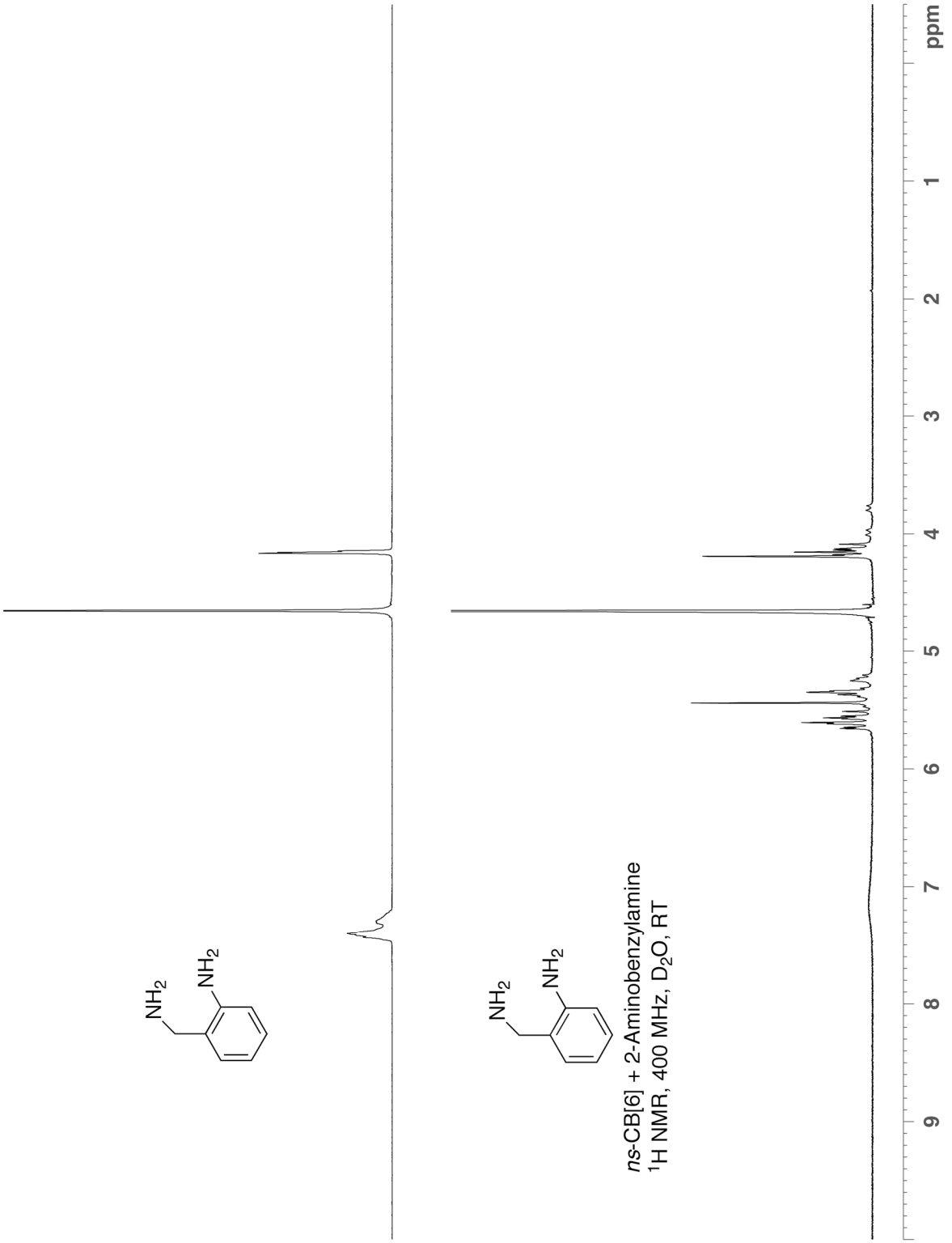

Figure S19. ^{1}H NMR spectrum recorded for 2-aminobenzylamine and its complex with *ns*-CB[6] (400 MHz, D_2O, RT).

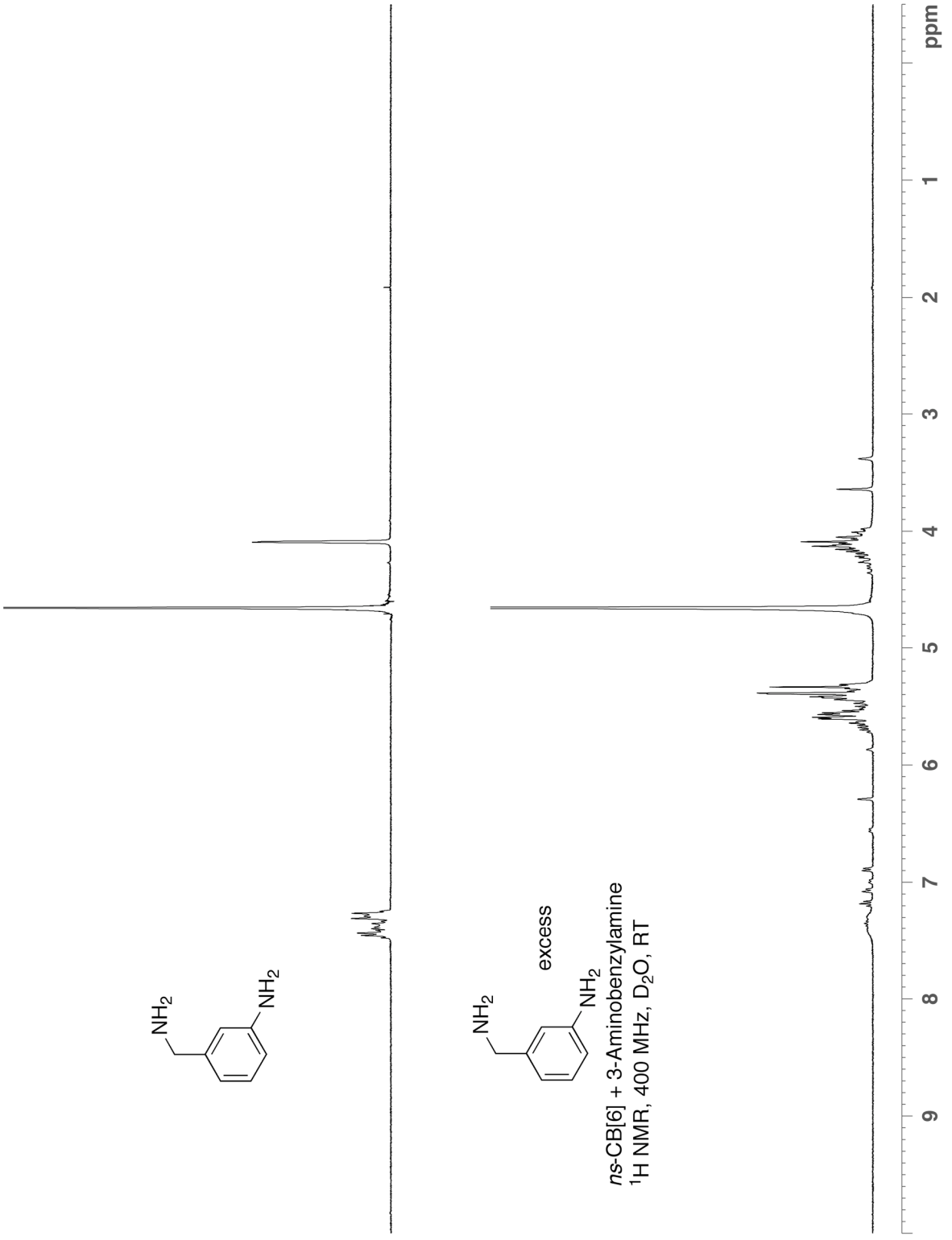

Figure S20. ^{1}H NMR spectrum recorded for 3-aminobenzylamine and its complex with *ns*-CB[6] (400 MHz, D_2O, RT). The ratio of the two diastereomers is 58:42.

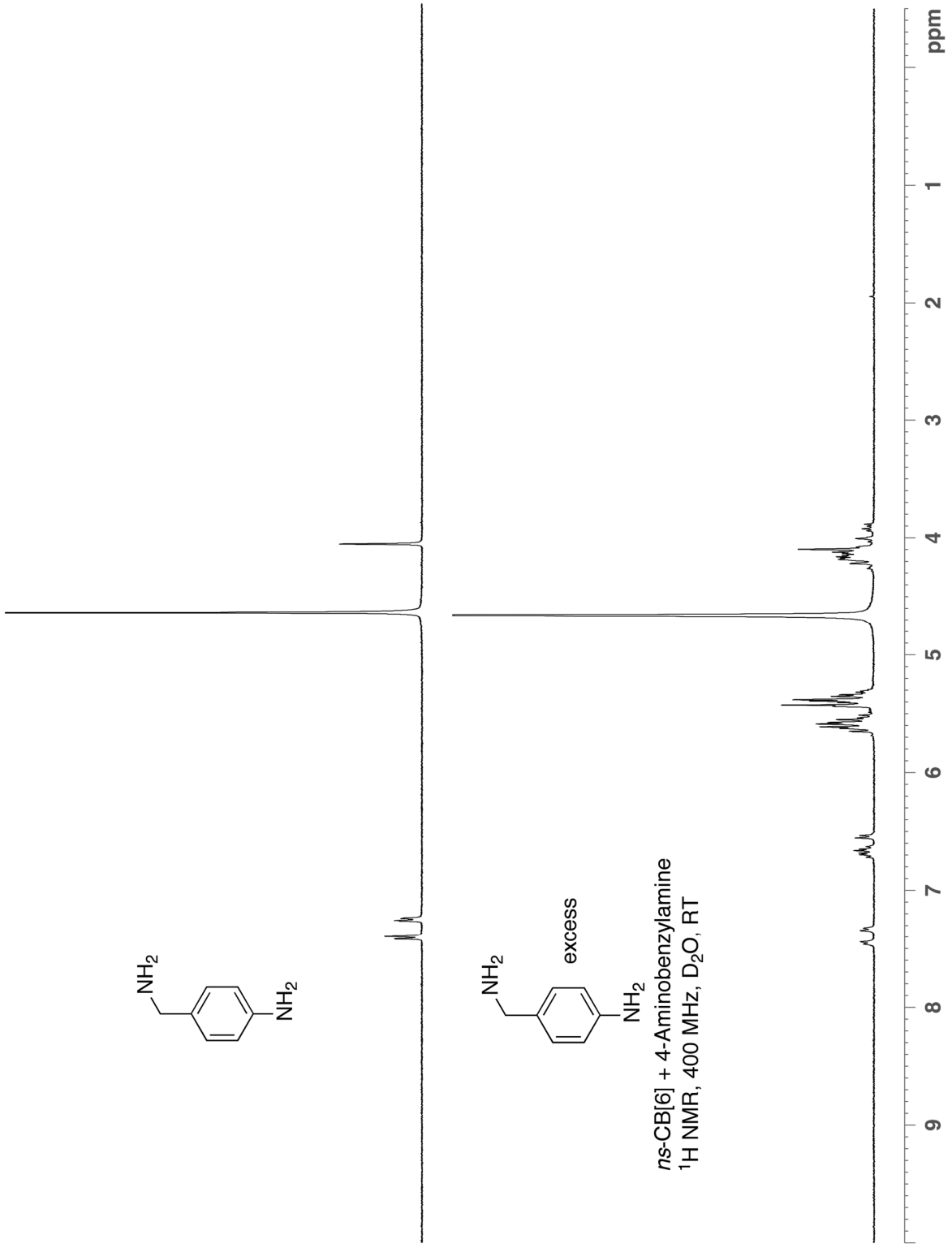

Figure S21. ^{1}H NMR spectra recorded for 4-aminobenzylamine and its complex with *ns*-CB[6] (400 MHz, D_2O, RT). The ratio of the two diastereomers is 72:28.

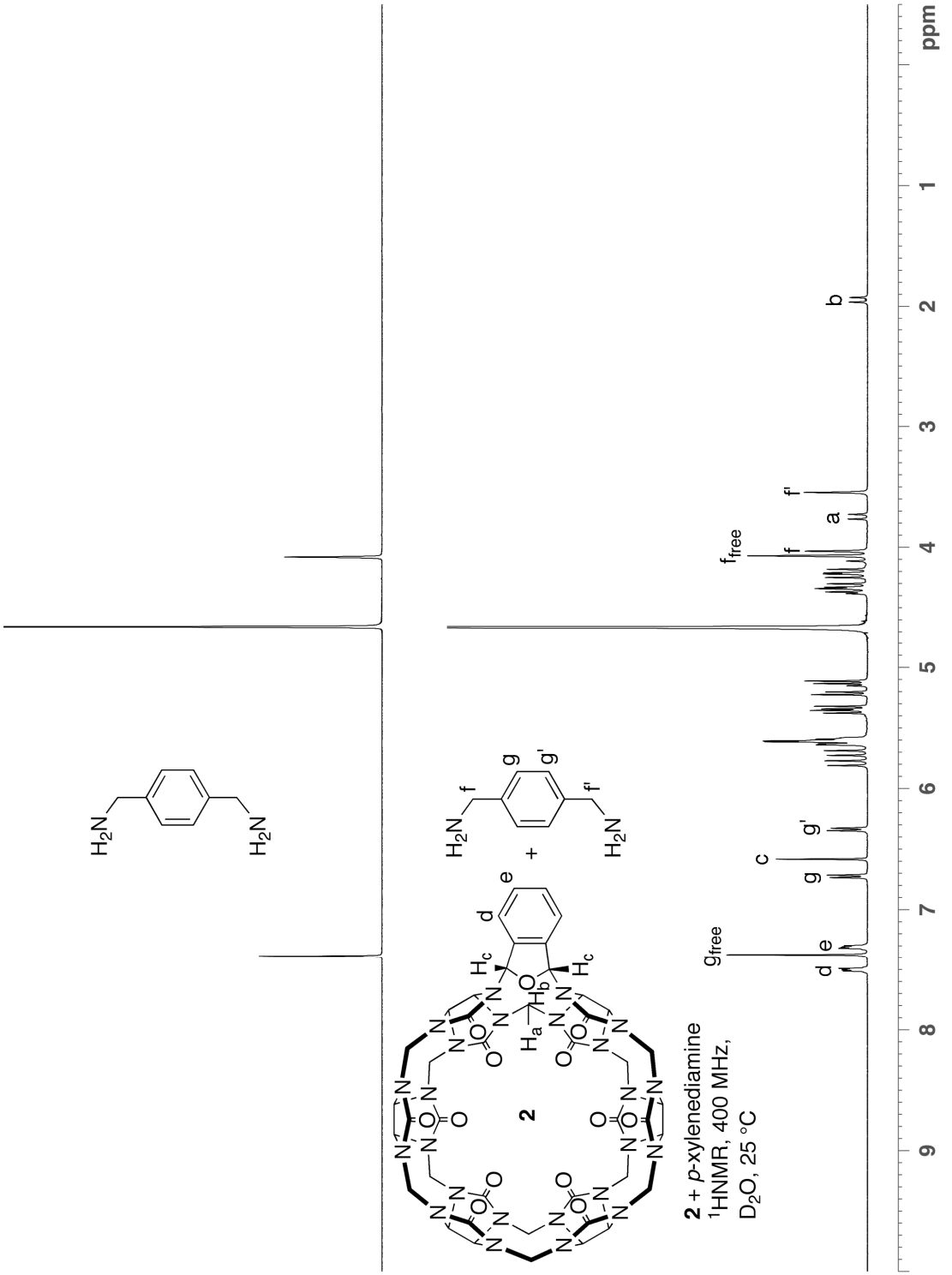

Figure S22. [1]H NMR spectra recorded for *p*-xylenediamine and its complex with **2** (400 MHz, D_2O, RT).

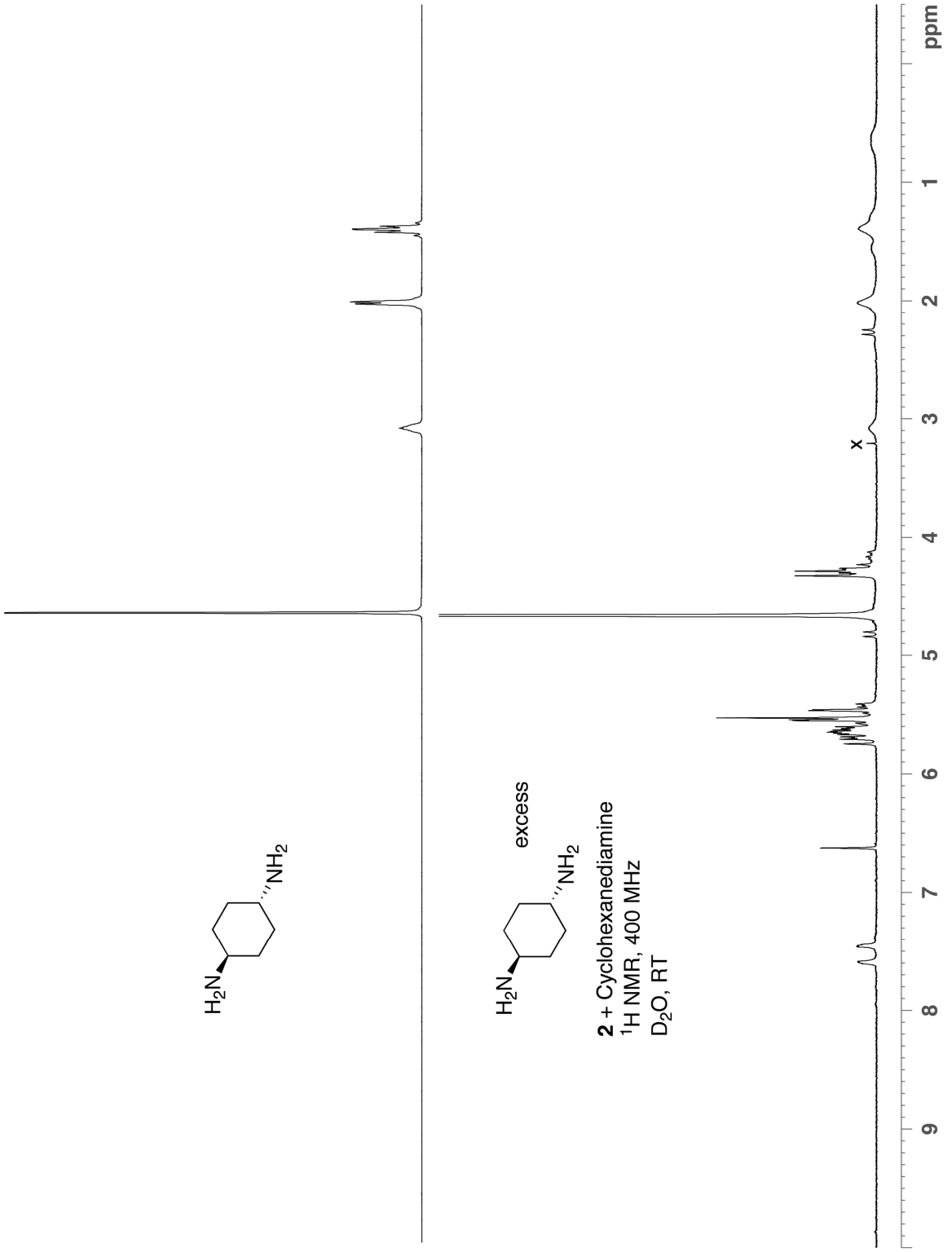

Figure S23. ^{1}H NMR spectra recorded for cyclohexanediamine and its complex with **2** (400 MHz, D_2O, RT, x = trace MeOH impurity).

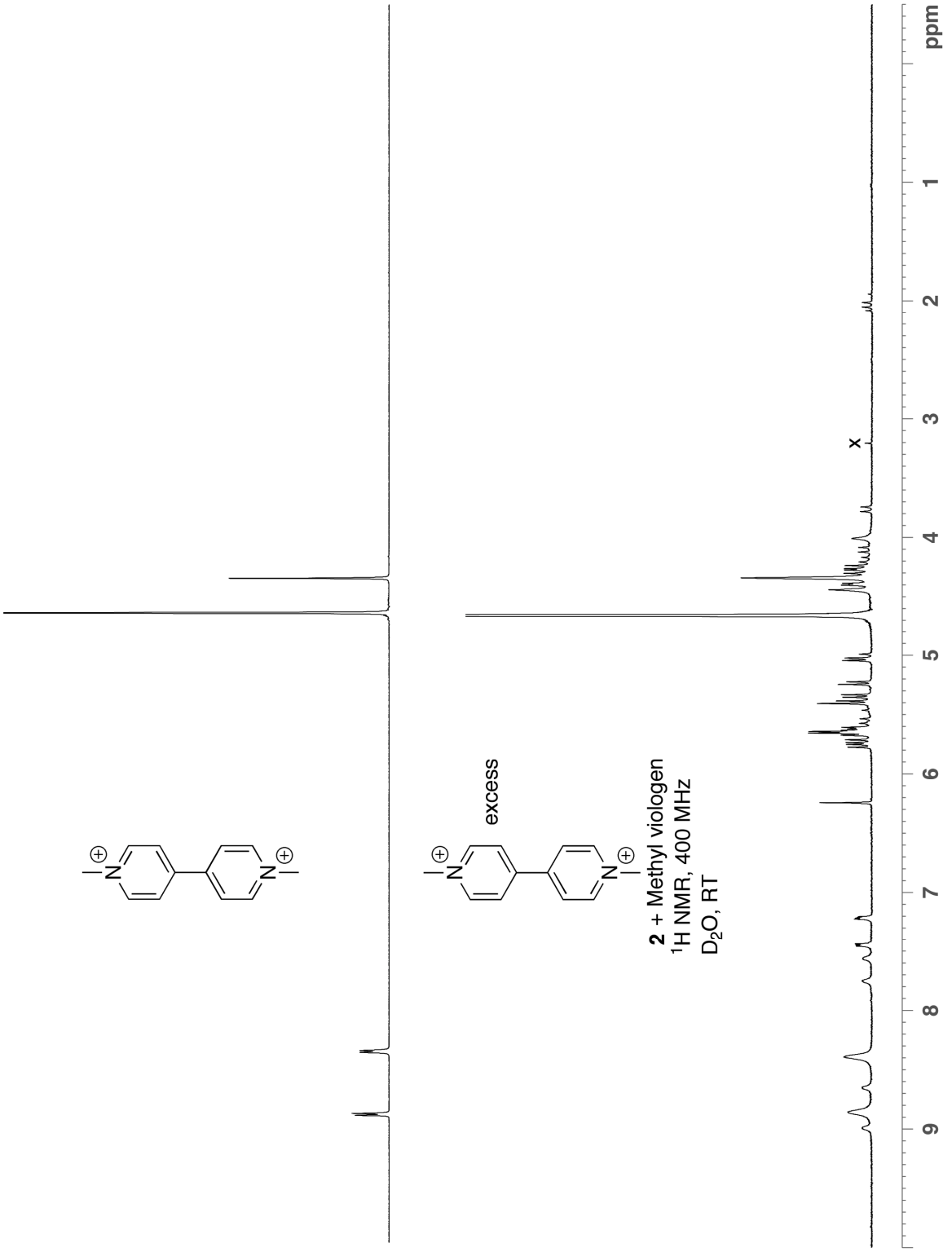

Figure S24. ^{1}H NMR spectra recorded for methyl viologen and its complex with **2** (400 MHz, D_2O, RT, x = trace MeOH impurity).

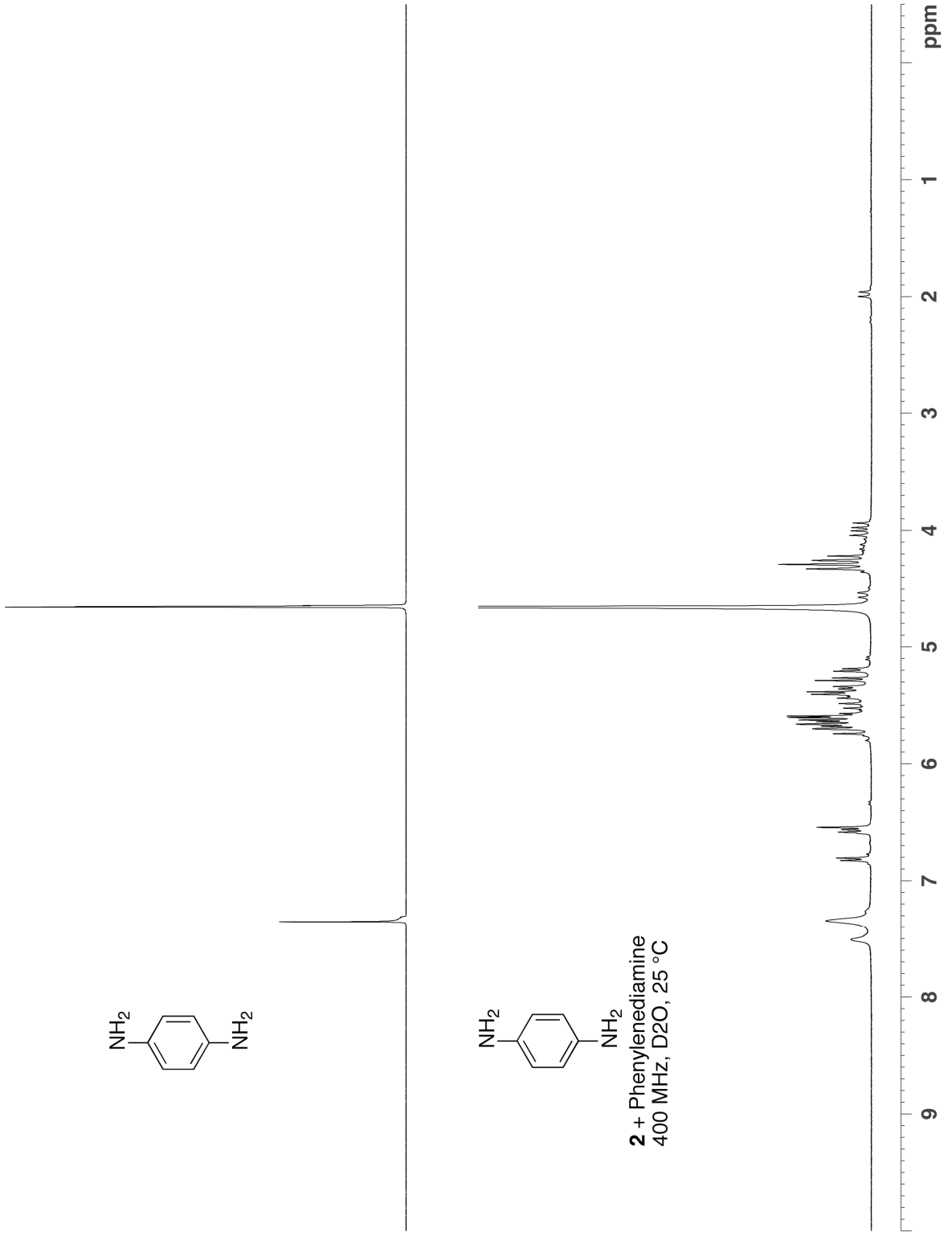

Figure S25. ^{1}H NMR spectra recorded for phenylenediamine and its complex with **2** (400 MHz, D_2O, RT).

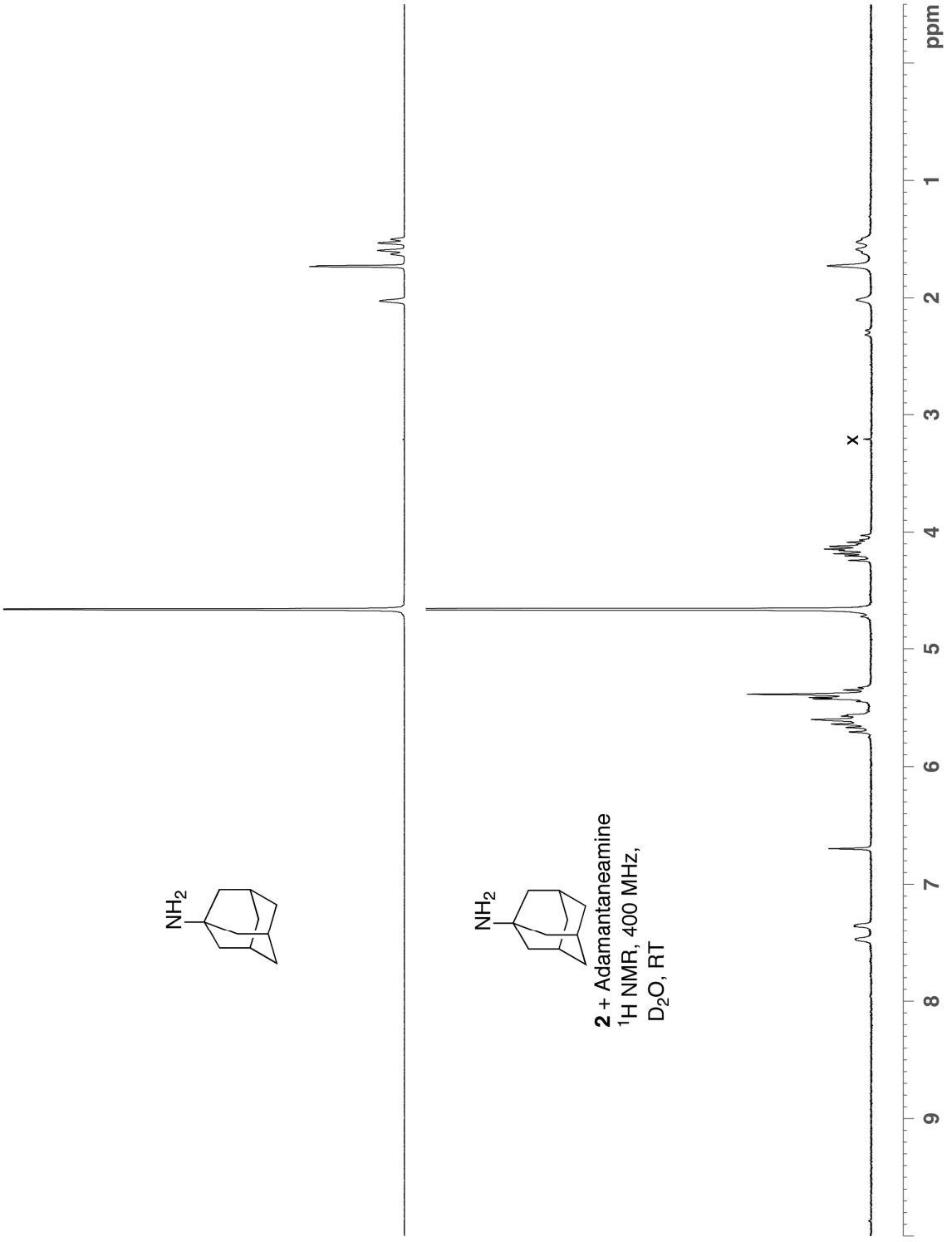

Figure S26. ^{1}H NMR spectra recorded for adamantaneamine and as a mixture with **2** (400 MHz, D_2O, RT, x = trace MeOH impurity).

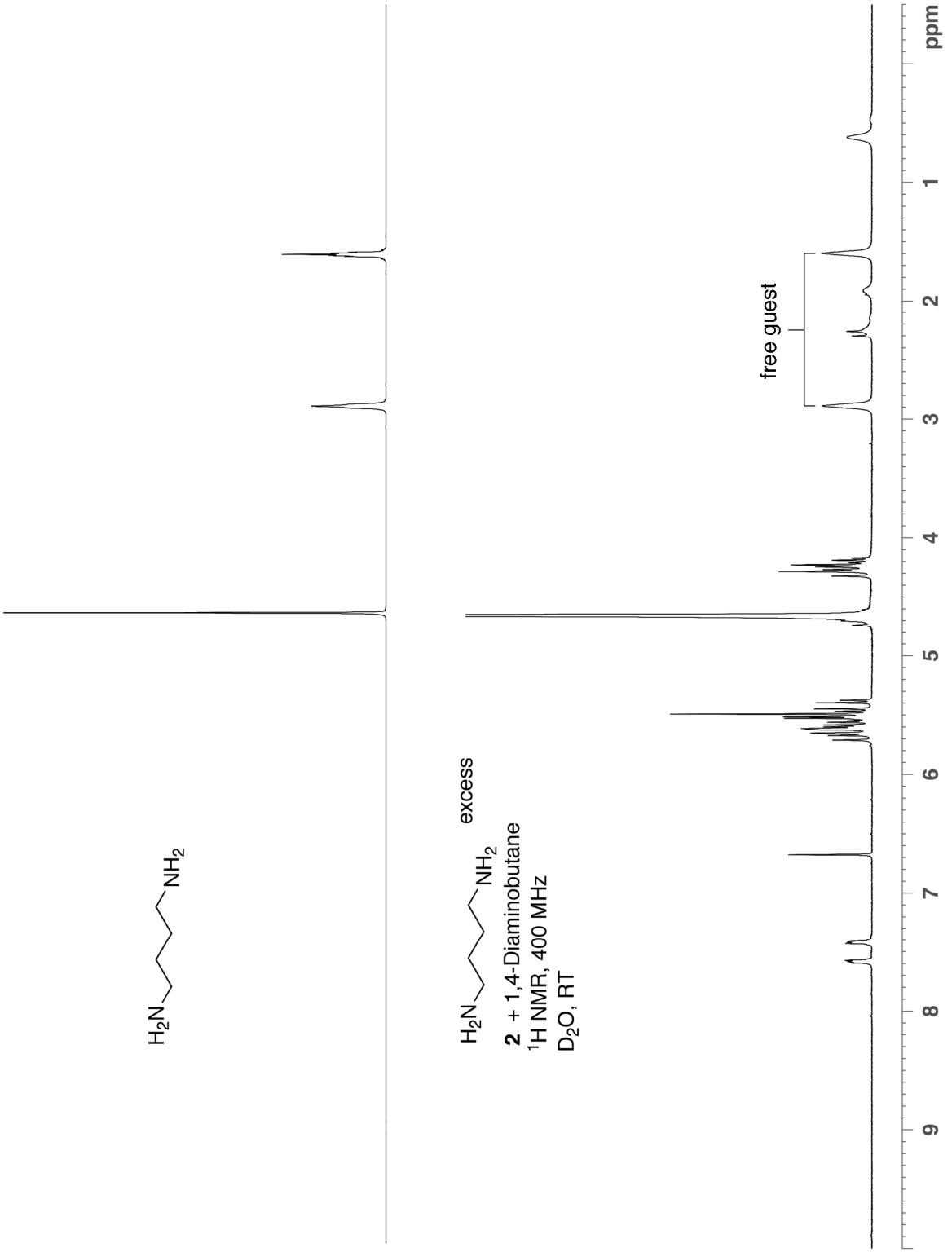

Figure S27. ^{1}H NMR spectra recorded for 1,4-diaminobutane and its complex with **2** (400 MHz, D_2O, RT).

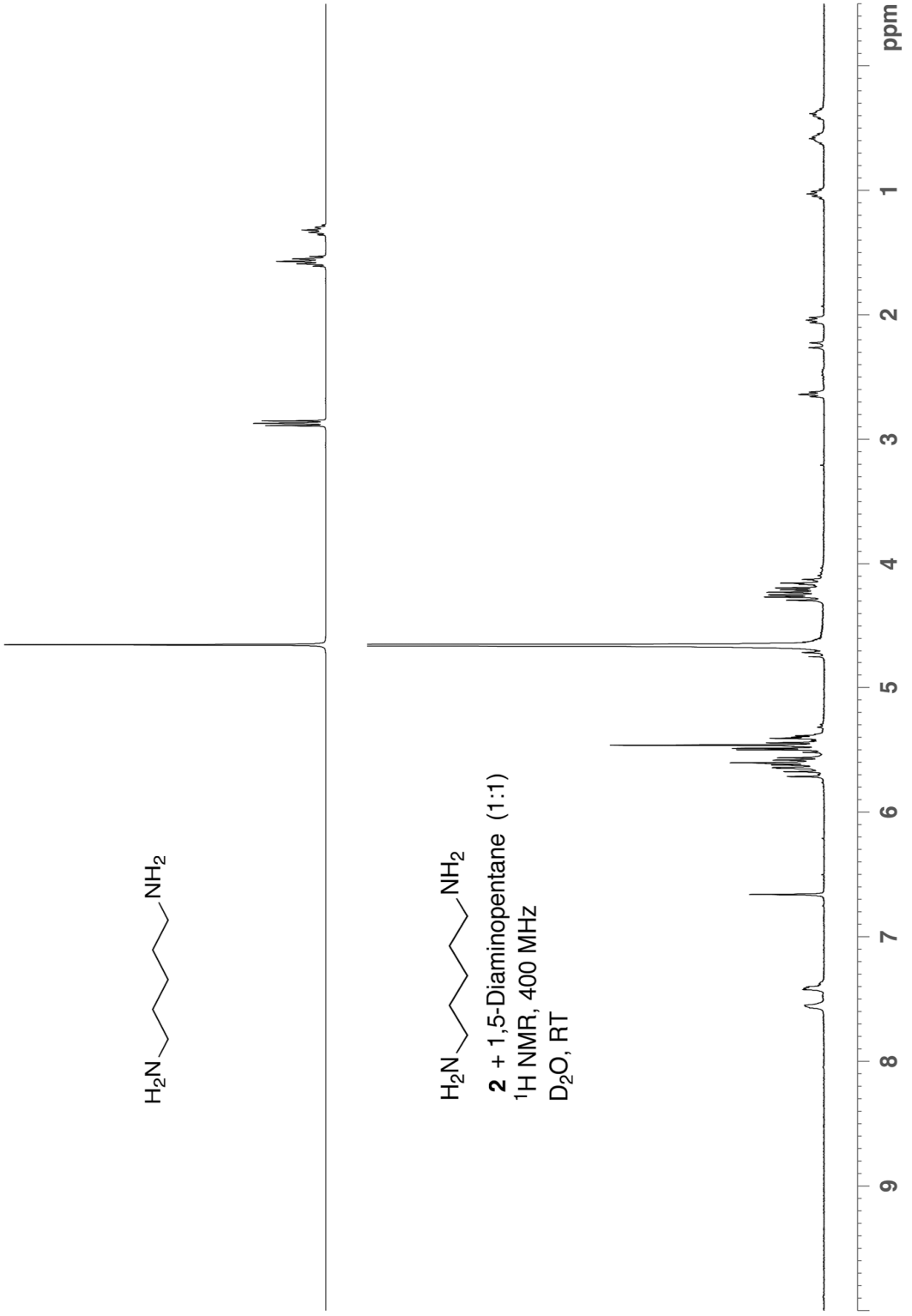

Figure S28. ^{1}H NMR spectra recorded for 1,5-diaminopentane and its complex with **2** (400 MHz, D_2O, RT).

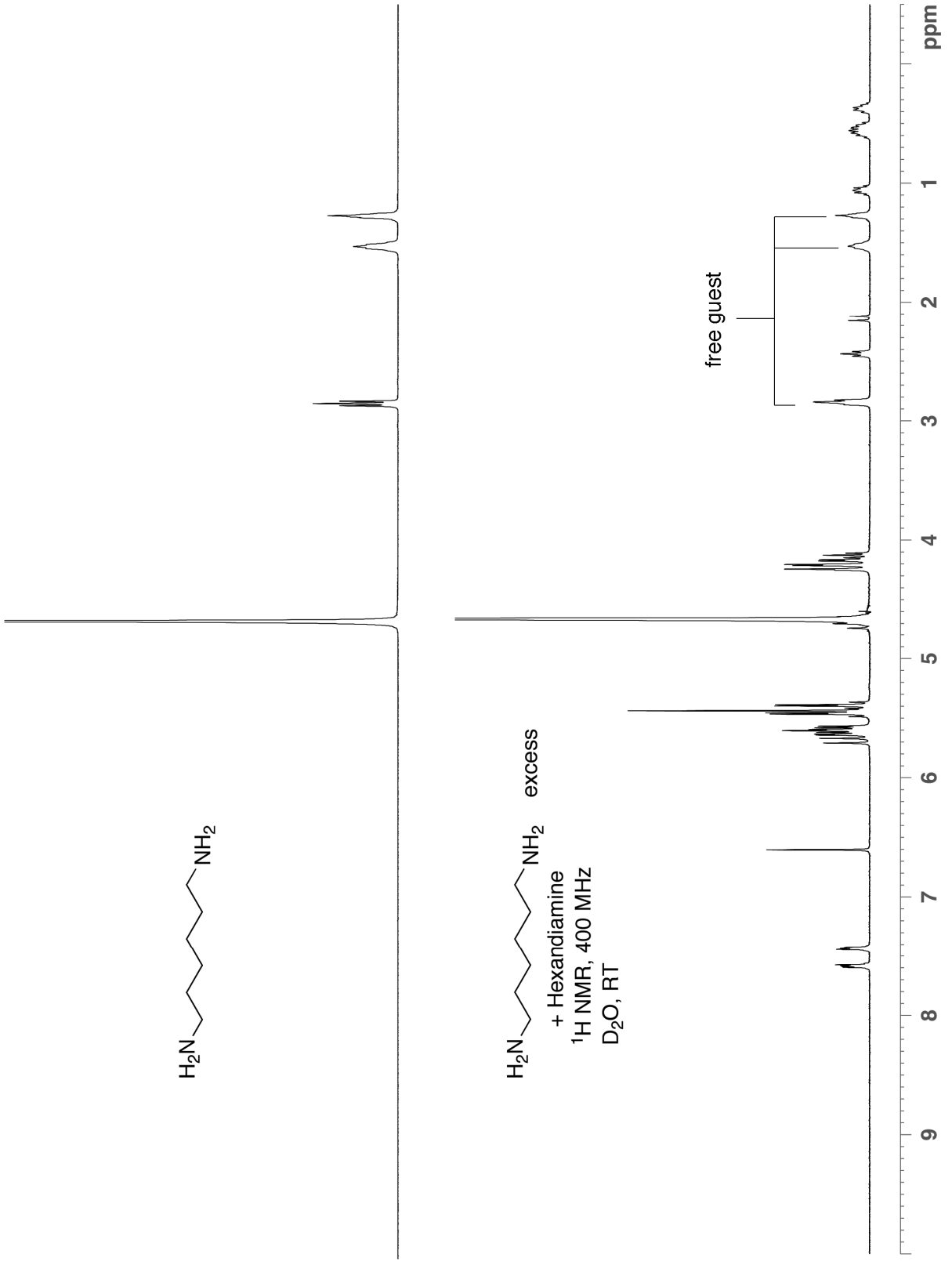

Figure S29. ^{1}H NMR spectra recorded for hexanediamine and its complex with **2** (400 MHz, D_2O, RT).

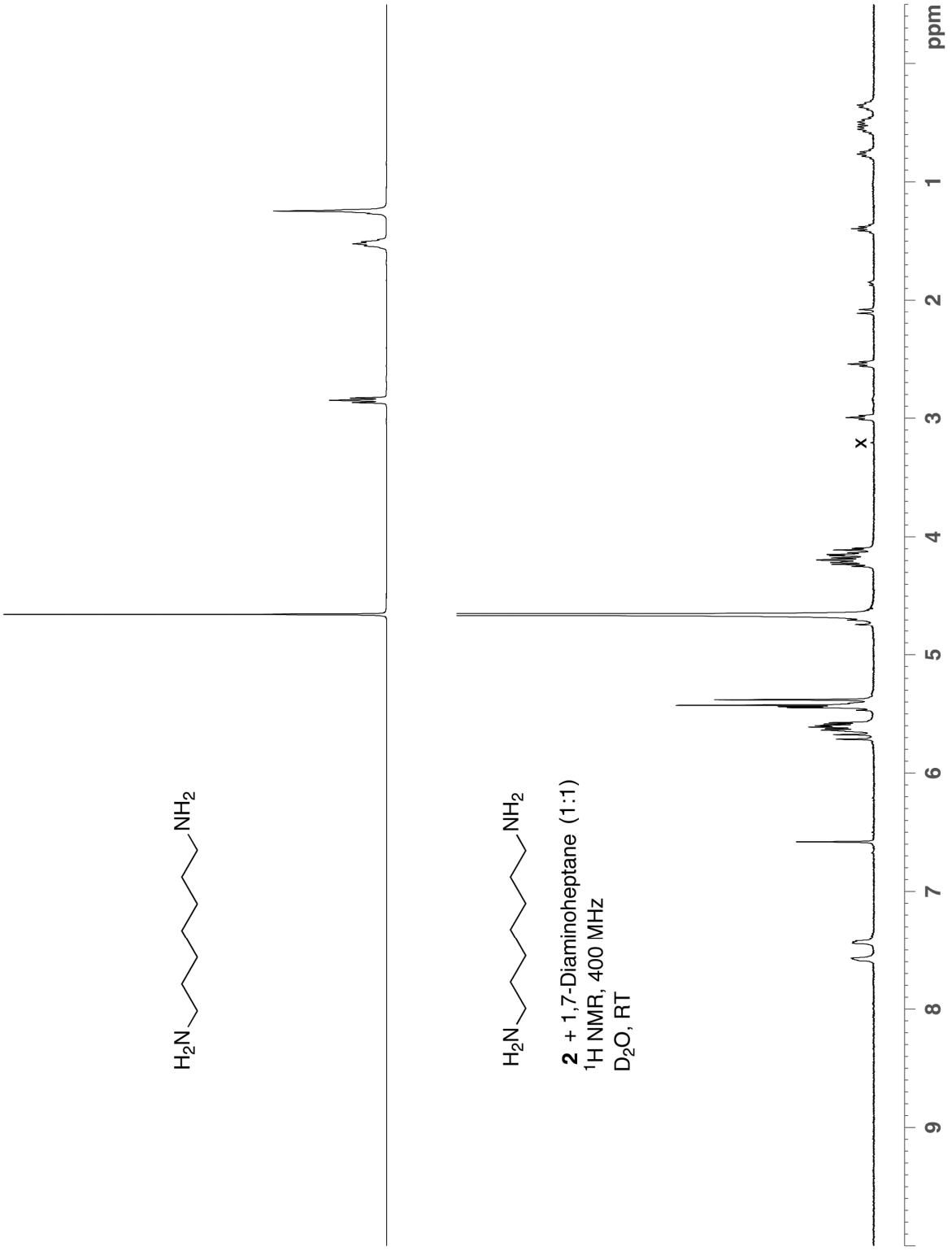

Figure S30. ^{1}H NMR spectra recorded for 1,7-diaminoheptane and its complex with **2** (400 MHz, D_2O, RT, x = trace MeOH impurity).

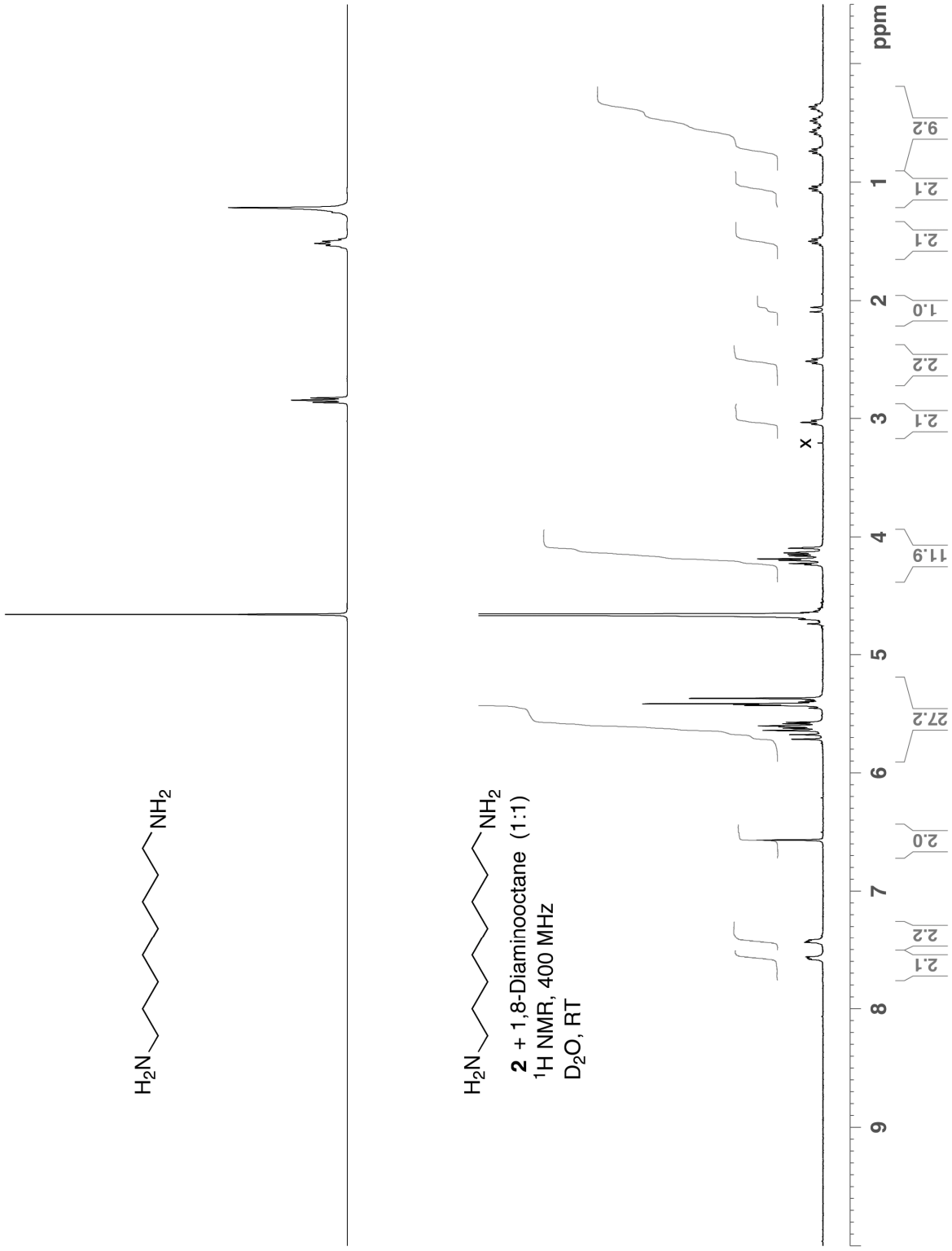

Figure S31. ^{1}H NMR spectra recorded for 1,8-diaminooctane and its complex with **2** (400 MHz, D_2O, RT, x = trace MeOH impurity).

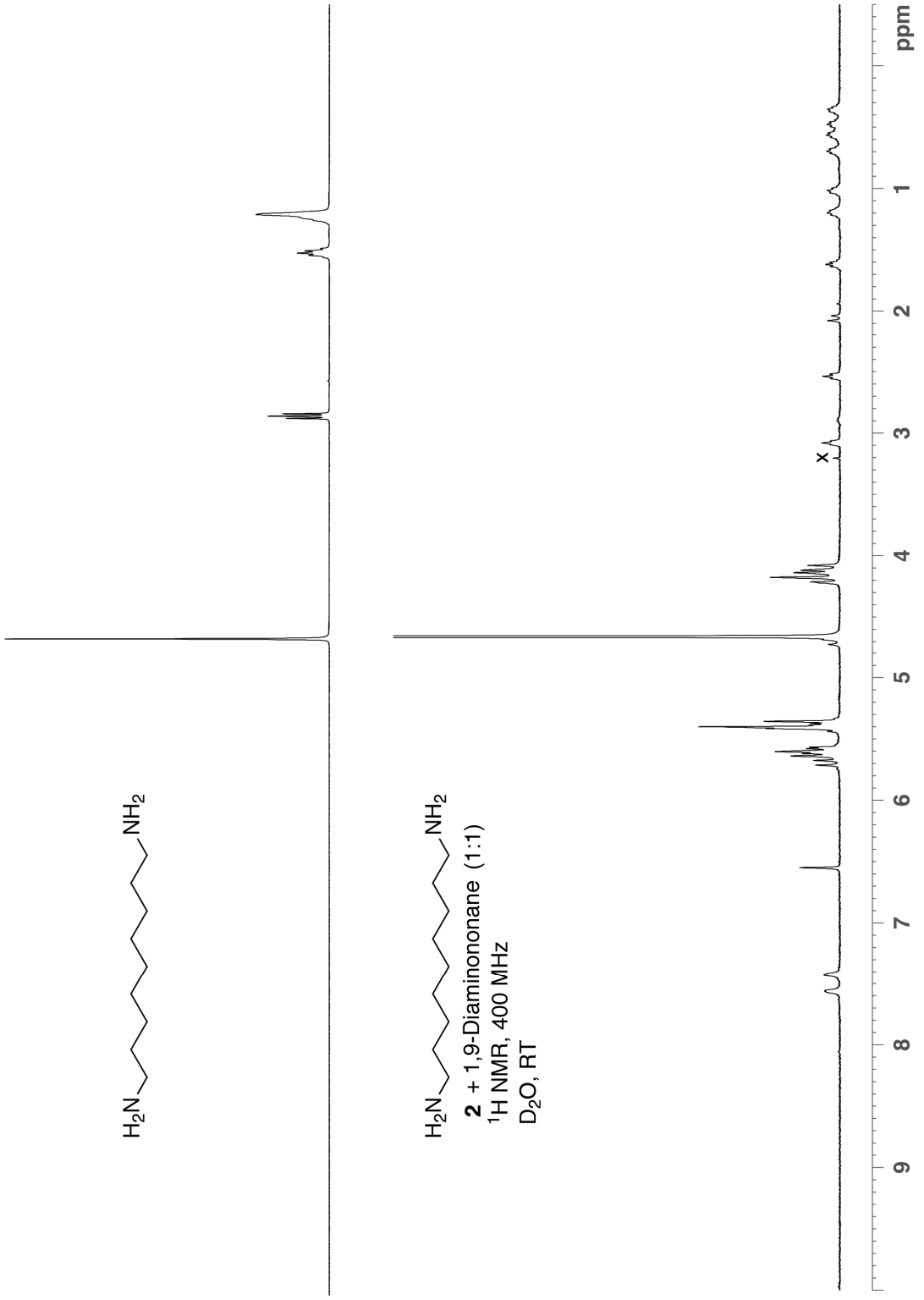

Figure S32. ^{1}H NMR spectra recorded for 1,9-diaminononane and its complex with **2** (400 MHz, D_2O, RT, x = trace MeOH impurity).

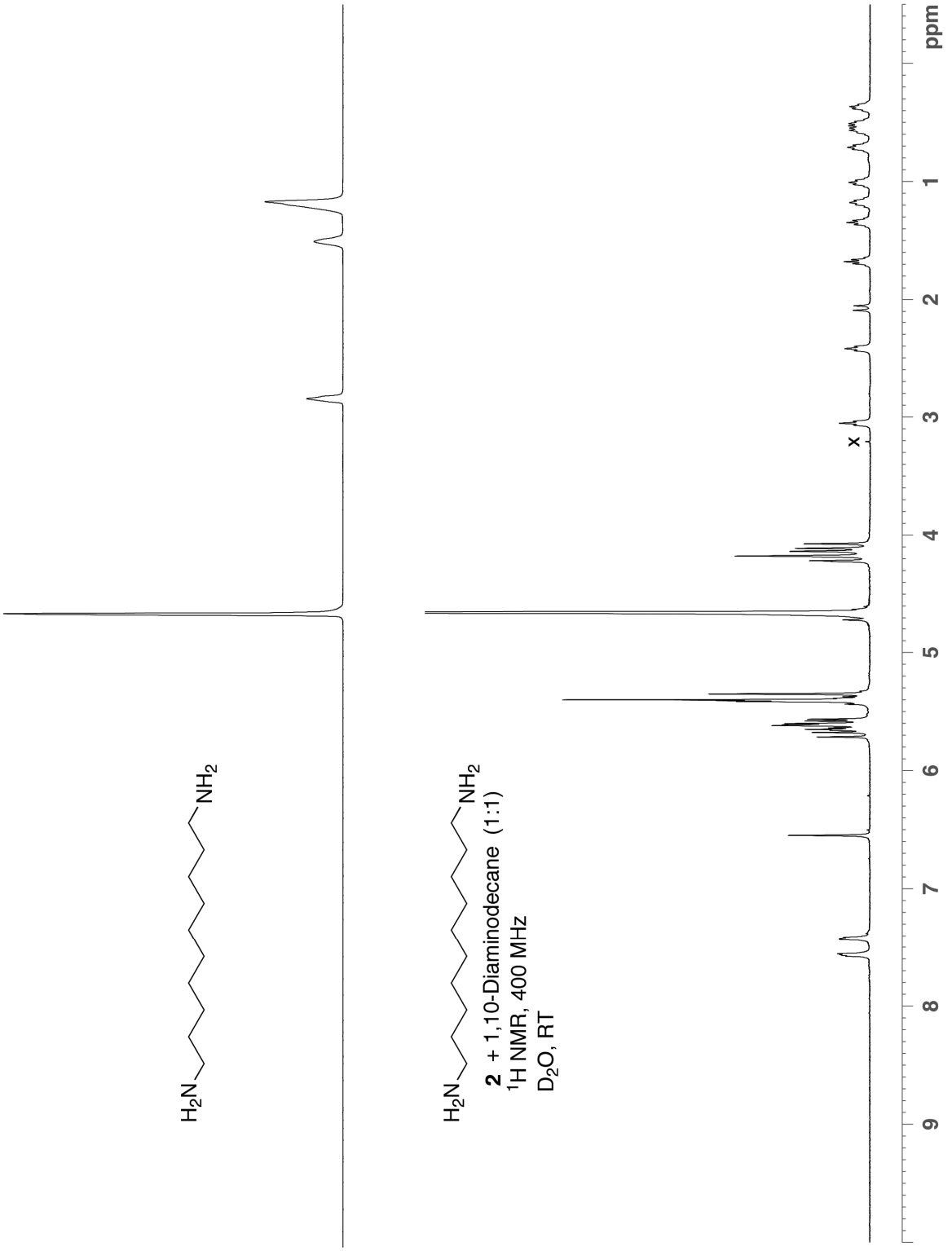

Figure S33. ^{1}H NMR spectra recorded 1,10-diaminodecane and its complex with **2** (400 MHz, D_2O, RT, x = trace MeOH impurity).

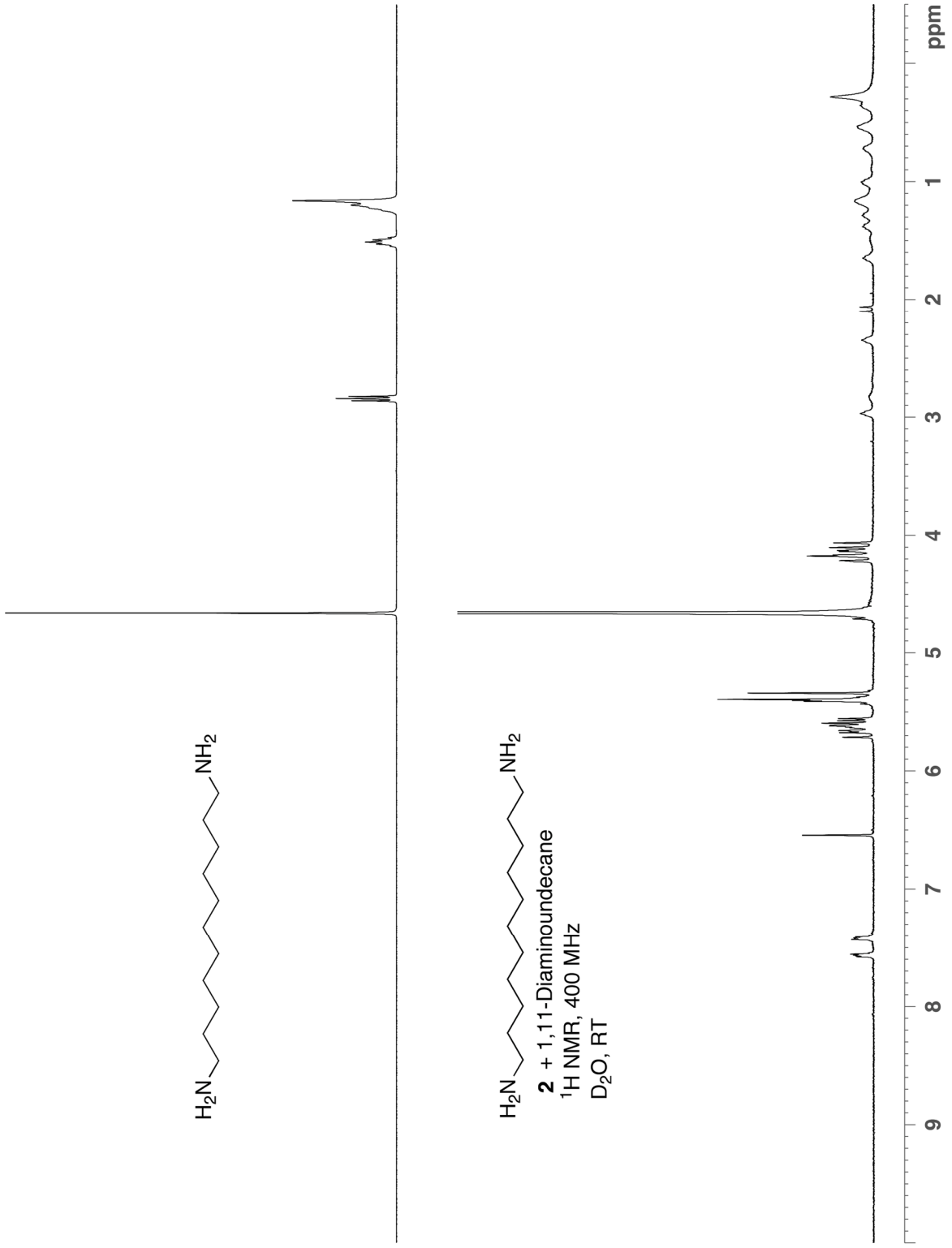

Figure S34. ^{1}H NMR spectra recorded 1,11-diaminoundecane and its complex with **2** (400 MHz, D_2O, RT).

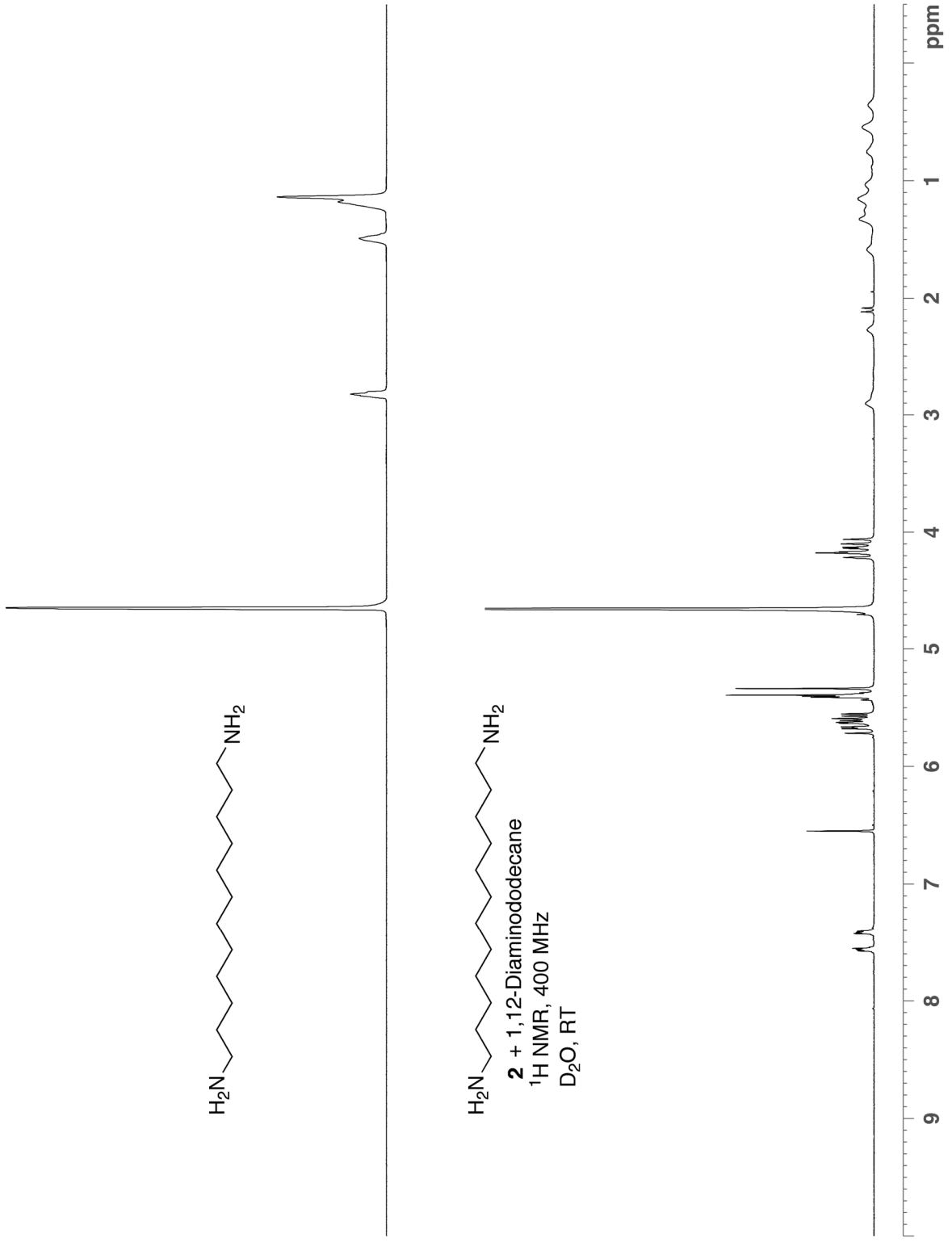

Figure S35. ^{1}H NMR spectra recorded for 1,12-diaminododecane and its complex with **2** (400 MHz, D_2O, RT).

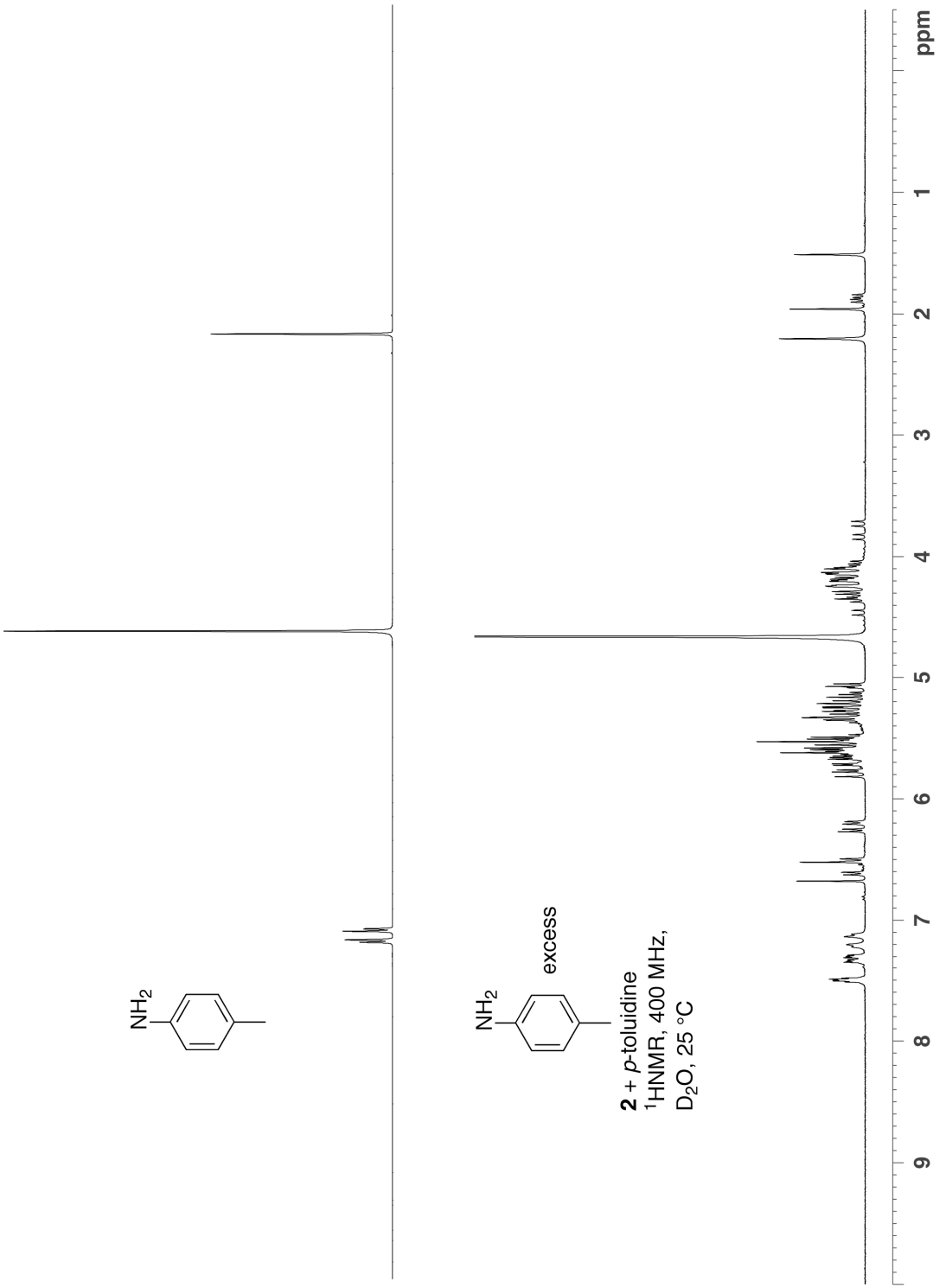

Figure S36. ^{1}H NMR spectra recorded for *p*-toluidine and its complex **2** (400 MHz, D_2O, RT).

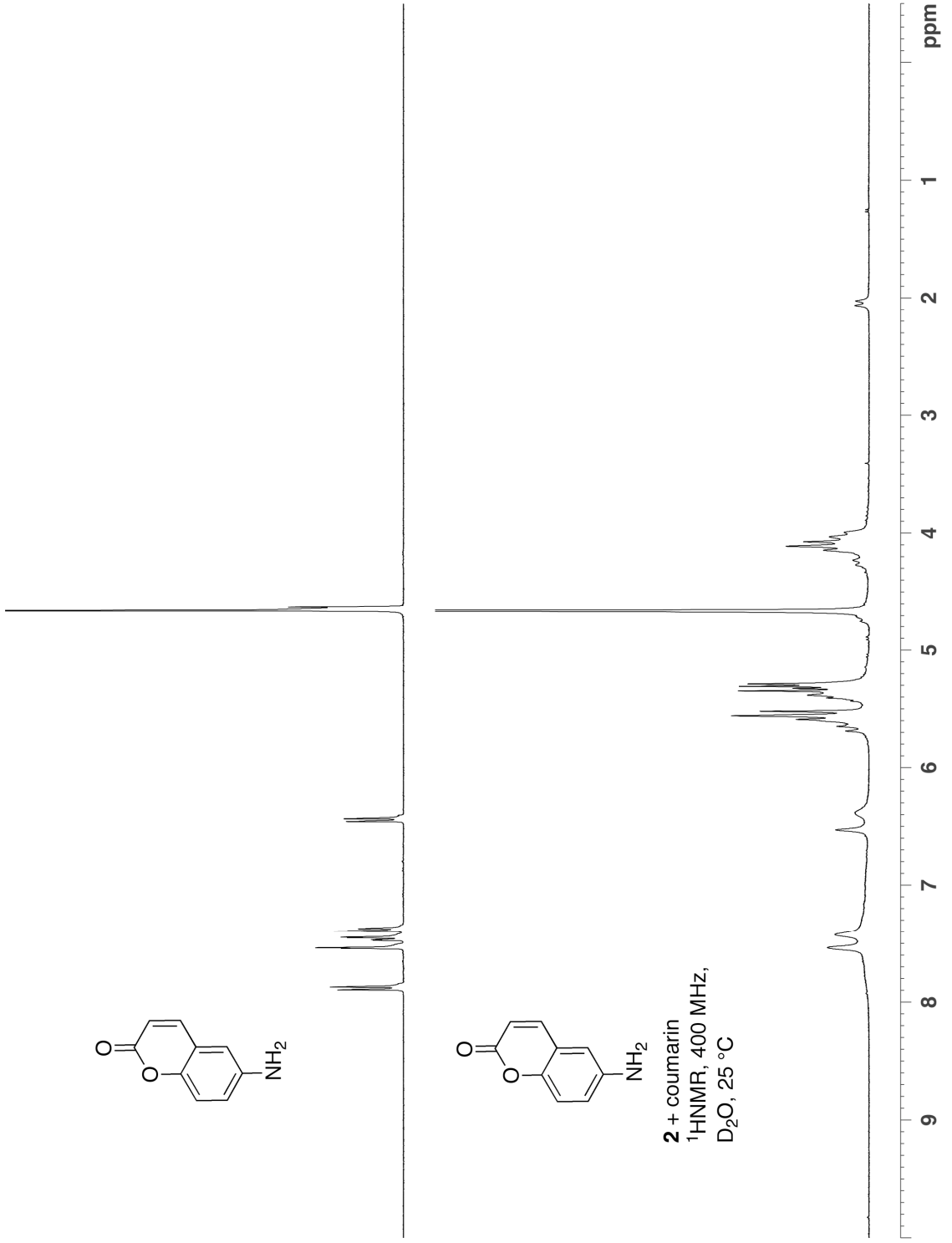

Figure S37. ^{1}H NMR spectra recorded for coumarin and its complex **2** (400 MHz, D_2O, RT).

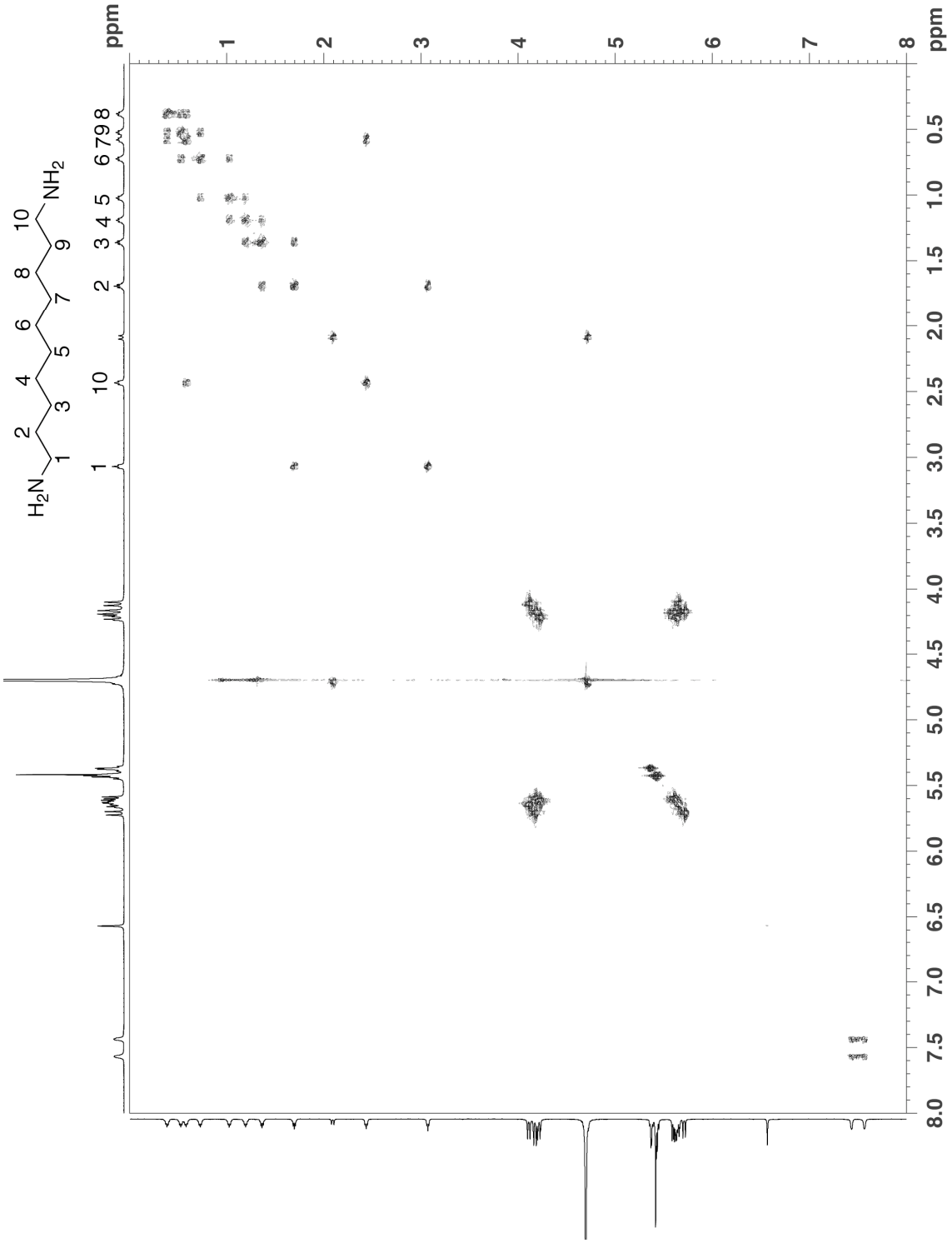

Figure S38. ^{1}H-^{1}H COSY NMR spectrum recorded for **2**•1,10-diaminodecane (600 MHz, D_2O, RT).

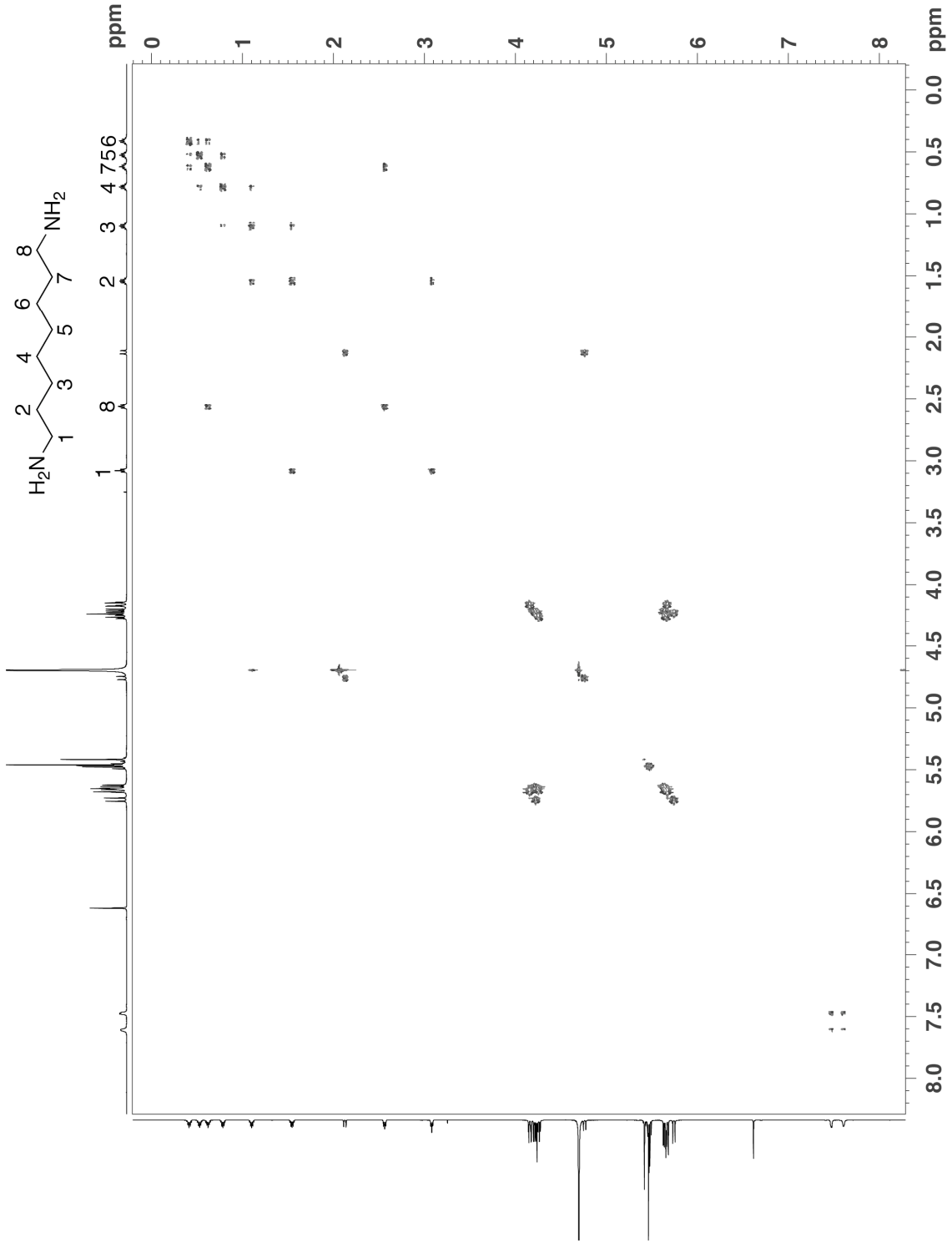

Figure S39. ^{1}H-^{1}H COSY NMR spectrum recorded for **2**•1,8-diaminooctane (600 MHz, D_2O, RT).

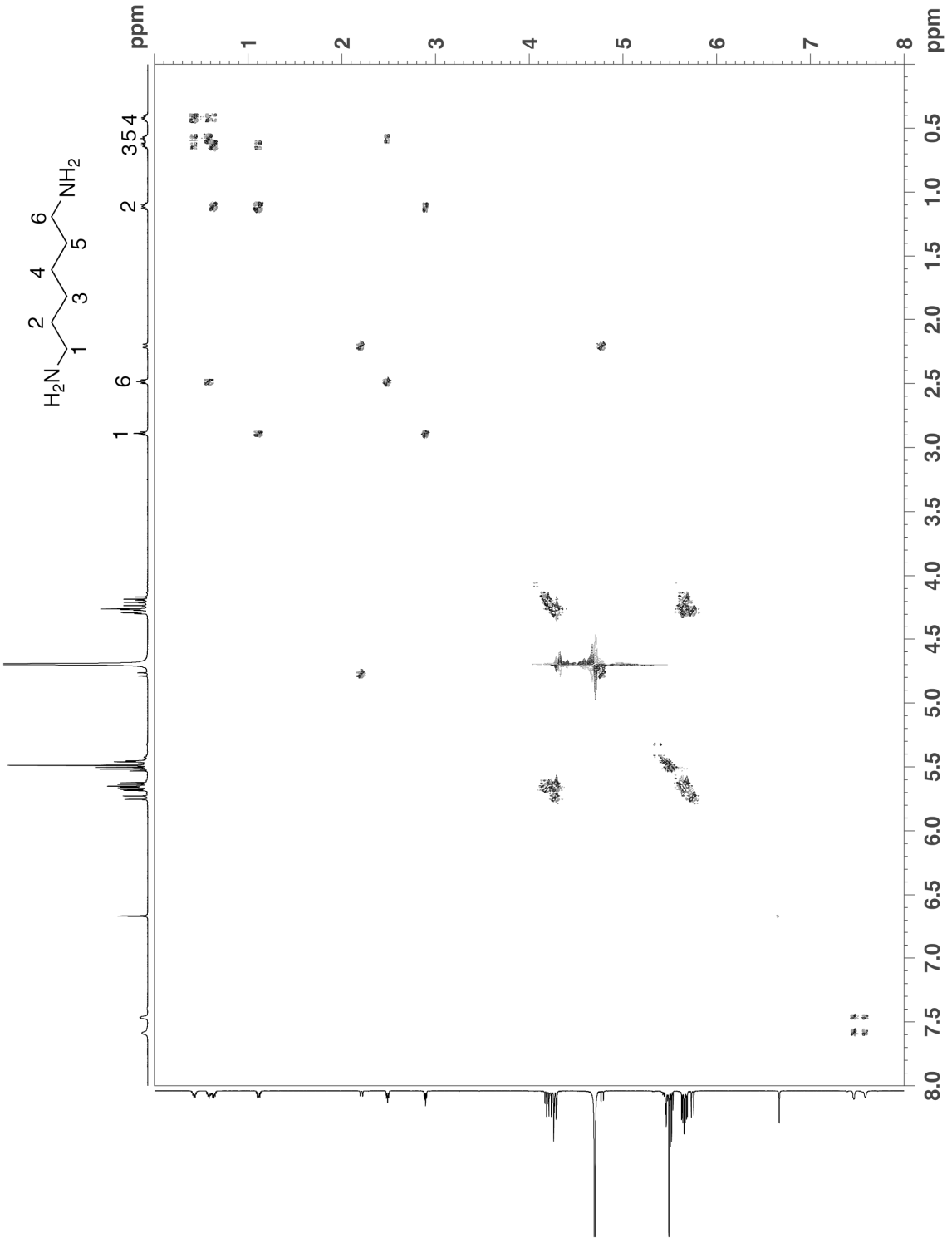

Figure S40. ^{1}H-^{1}H COSY NMR spectrum recorded for **2**•1,6-diaminohexane (600 MHz, D_2O, RT).

Crystal Structure Information for UM # 1574

Issued by: Peter Y. Zavalij

Crystal No. & ID	:	**1574**: Compound **2**
Compound name	:	$[K(H_2O)_2(CB6')_2 \cdot 2TFAH](TFA) \cdot \sim 4TFAH \cdot \sim 13H_2O$
Chemical formula	:	$KC_{100}H_{116}F_{21}N_{48}O_{55}$
Final R_1 [I>2σ(I)]	:	**5.37 %**

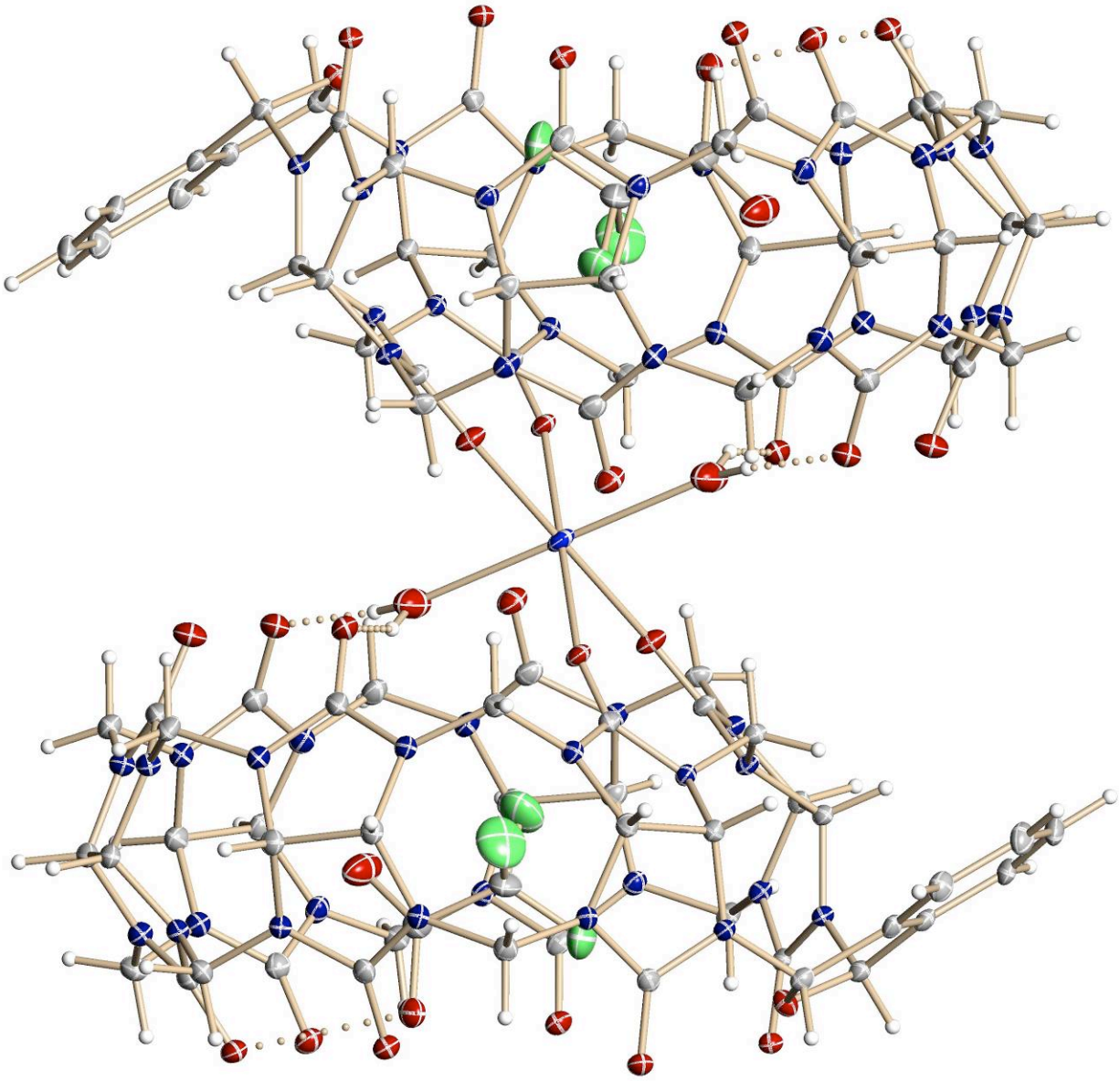

Figure S41. A view of compound **2** showing the numbering scheme employed. Anisotropic atomic displacement ellipsoids for the non-hydrogen atoms are shown at the 30% probability level. Hydrogen atoms are displayed with an arbitrarily small radius.

A colorless prism of $KC_{100}H_{116}F_{21}N_{48}O_{55}$, approximate dimensions 0.095×0.15×0.40 mm^3, was used for the X-ray crystallographic analysis. The X-ray intensity data were measured at 150(2) K on a three-circle diffractometer system equipped with Bruker Smart Apex II CCD area detector using a graphite monochromator and a MoKα fine-focus sealed tube (λ= 0.71073 Å) . The detector was placed at a distance of 5.8 cm from the crystal.

A total of 2491 frames were collected with a scan width of 0.3° an exposure time of 20 sec/frame using Apex2 (Bruker, 2005). The total data collection time was 18 hours. The frames were integrated with Apex2 software package using a narrow-frame integration algorithm. The integration of the data using a Monoclinic unit cell yielded a total of 66732 reflections to a maximum θ angle of 25.00°, of which 12908 were independent (completeness = 99.9%, R_{int} = 3.86%, R_{sig} = 3.22%) and 9287 were greater than 2σ(I). The final cell dimensions of a = 31.0746(11) Å, b = 16.9744(6) Å, c = 28.0904(10) Å, α = 90°, β = 97.9680(10)°, γ = 90°, V = 14673.9(9) $Å^3$, are based upon the refinement of the XYZ-centroids of 16943 reflections with 2.3 < θ < 28.0° using Apex2 software. Analysis of the data showed 0 % decay during data collection. Data were corrected for absorption effects with the Semi-empirical from equivalents method using SADABS (Sheldrick, 1996). The minimum and maximum transmission coefficients were 0.917 and 0.984.

The structure was solved and refined using the SHELXS-97 (Sheldrick, 1990) and SHELXL-97 (Sheldrick, 1997) software in the space group *C2/c* with Z = 4 for the formula unit $KC_{100}H_{116}F_{21}N_{48}O_{55}5$. The final anisotropic full-matrix least-squares refinement on F^2 with 925 variables converged at R_1 = 5.37 % for the observed data and wR_2 = 10.48 % for all data. The goodness-of-fit was 1.000. The largest peak on the final difference map was 0.618$\bar{e}$/$Å^3$ and the largest hole was -0.697$\bar{e}$/$Å^3$. On the basis of the final model, the calculated density was 1.498 g/cm^3 and F(000), 6800$\bar{e}$.

Overall structure quality considerations:

1. Strong data set, no disorder, R_1 4% maximum. Publishable quality.
2. **Good data set, perhaps some minor disorder, R_1 6% maximum. Publishable quality.**
3. Average data set and/or easily modeled disorder or twinning. Publishable with care.
4. Weak data and/or major disorder or twinning that is not easily modeled. Publishable in some cases.
5. Very weak data and/or unexplained features of data or model. Not of publishable quality.

A structure with a quality factor of 4 or 5 should not be used for a regulatory document without prior consultation.

Comments:

- Data quality:	very good
- Twinning:	none
- Disorder:	solvent TFA and water, removed using Squeeze from Platon
- H-atoms:	constrained geometry as riding on attached atom (A)
	U_{iso}(H)=1.5U_{iso}(A) for CH_3 and 1.2U_{iso}(A) for other groups
- Residual density:	near disordered groups
- Structure quality:	good
Publishable	Yes

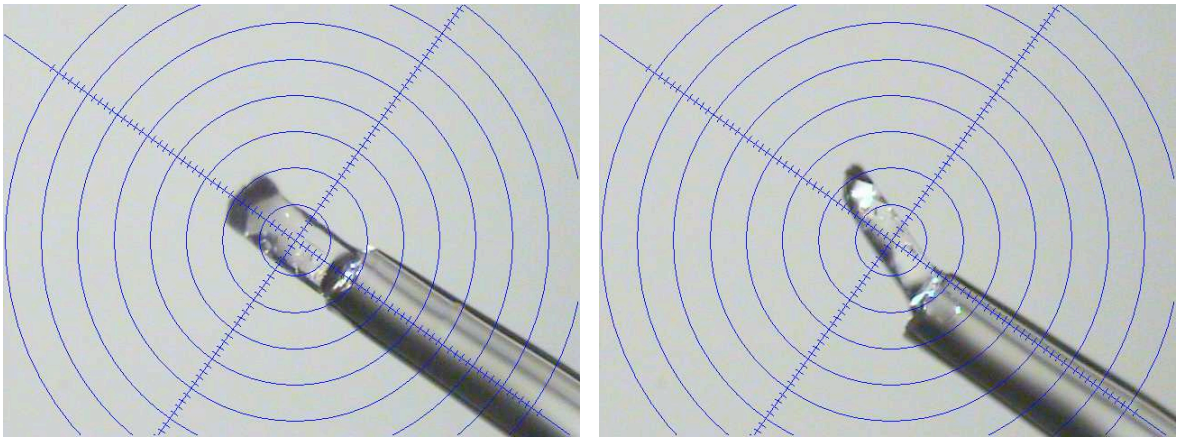

Table S1. Crystal data and structure refinement for compound **2**.

X-ray lab book No.		1574
Crystal ID		compound **2**
Empirical formula		$KC_{100}H_{116}F_{21}N_{48}O_{55}$
Formula weight		3308.51
Temperature		150(2) K
Wavelength		0.71073 Å
Crystal size		0.40×0.15×0.095 mm^3
Crystal habit		colourless prism
Crystal system		Monoclinic
Space group		C2/c
Unit cell dimensions		a = 31.0746(11) Å α = 90°
		b = 16.9744(6) Å β = 97.9680(10)°
		c = 28.0904(10) Å γ = 90°
Volume		14673.9(9) $Å^3$
Z		4
Density, ρ_{calc}		1.498 g/cm^3
Absorption coefficient, μ		0.166 mm^{-1}
F(000)		6800ē
Diffractometer		Bruker Smart Apex II CCD area detector
Radiation source		fine-focus sealed tube, MoKα
Detector distance		5.8 cm
Data collection method		ω and scans
Total frames		2491
Frame size		1024 pixels
Frame width		0.3°
Exposure per frame		20 sec
Total measurement time		18 hours
θ range for data collection		1.32 to 25.00°
Index ranges		$-33 \le h \le 36$, $-20 \le k \le 20$, $-33 \le l \le 33$
Reflections collected		66732
Independent reflections		12908
Observed reflection, I>2σ(I)		9287
Coverage of independent reflections		99.9 %
Variation in check reflections		0 %
Absorption correction		Semi-empirical from equivalents
		SADABS (Sheldrick, 1996)
Max. and min. transmission		0.984 and 0.917
Structure solution technique		direct
Structure solution program		SHELXS-97 (Sheldrick, 1990)
Refinement technique		Full-matrix least-squares on F^2
Refinement program		SHELXL-97 (Sheldrick, 1997)
Function minimized		$\Sigma w(F_o^2 - F_c^2)^2$
Data / restraints / parameters		12908 / 256 / 925
Goodness-of-fit on F^2		1.067
Δ/σ_{max}		0.000
Final R indices:	R_1, I>2σ(I)	0.0537
	wR_2, all data	0.1048
	R_{int}	0.0386
	R_{sig}	0.0322
Weighting scheme		$w = 1/[\sigma^2(F_o^2)+ (0.002P)^2 + 46.6P]$,
		$P = [\max(F_o^2 ,0) + 2F_o^2]/3$
Largest diff. peak and hole		0.618 and -0.697ē/$Å^3$

$R_1 = \Sigma||F_o|-|F_c||/\Sigma|F_o|$, $wR_2 = [\Sigma w(F_o^2-F_c^2)^2/\Sigma w(F_o^2)^2]^{1/2}$

Crystal Structure Information for Complex 2•3f

Issued by: Peter Y. Zavalij

Crystal No. & ID	:	**1597**: complex **2•3f**
Compound name	:	complex **2•3f**
Chemical formula	:	$[(C_{43}H_{40}N_{24}O_{13})<(C_9H_{24}N_2)]I_2 \cdot 15H_2O$
Final R_1 [I>2σ(I)]	:	**7.23 %**

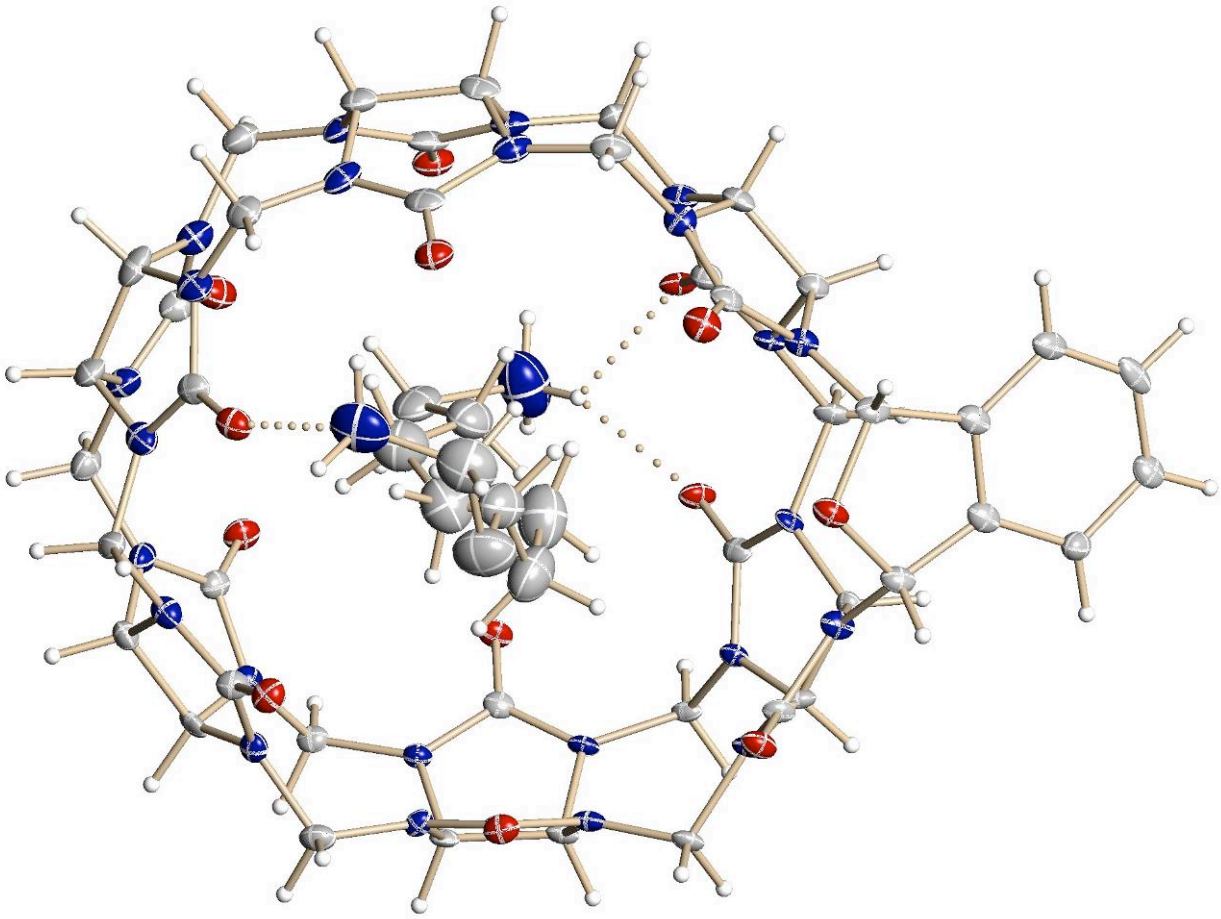

Figure S42. A view of complex **2•3f**. Anisotropic atomic displacement ellipsoids for the non-hydrogen atoms are shown at the 30% probability level. Hydrogen atoms are displayed with an arbitrarily small radius.

A yellow prism of $[(C_{43}H_{40}N_{24}O_{13})<(C_9H_{24}N_2)]I_2 \cdot 15H_2O$, approximate dimensions 0.195× 0.35× 0.39 mm^3, was used for the X-ray crystallographic analysis. The X-ray intensity data were measured at 150(2) K on a three-circle diffractometer system equipped with Bruker Smart Apex II CCD area detector using a graphite monochromator and a MoKα fine-focus sealed tube (λ= 0.71073 Å). The detector was placed at a distance of 6.00 cm from the crystal.

A total of 2035 frames were collected with a scan width of 0.3° in ω and an exposure time of 30 sec/frame using Apex2 (Bruker, 2005). The total data collection time was 20.1 hours. The frames were integrated with Apex2 software package using a narrow-frame integration algorithm. The integration of the data using a Cubic unit cell yielded a total of 134638 reflections to a maximum θ angle of 22.50°, of which 9175 were independent (completeness = 99.8%, R_{int} = 5.31%, R_{sig} = 2.37%) and 8432 were greater than 2σ(I). The final cell dimensions of *a* = 27.6038(2) Å, *b* = 27.6038(2) Å, *c* = 27.6038(2) Å, α= 90°, β= 90°, γ= 90°, *V* = 21033.3(3) $Å^3$, are based upon the refinement of the XYZ-centroids of 37157 reflections with 2.2 < θ < 21.0° using Apex2. Analysis of the data showed 0 % decay during data collection. Data were corrected for absorption effects with the Semi-empirical from equivalents method using SADABS (Sheldrick, 1996). The minimum and maximum transmission coefficients were 0.734 and 0.823.

The structure was solved and refined using the SHELXS-97 (Sheldrick, 1990) and SHELXL-97 (Sheldrick, 1997) software in the space group $P2_13$ with Z = 12 for the formula unit $C_{52}H_{94}I_2N_{26}O_{28}$. The final anisotropic full-matrix least-squares refinement on F^2 with 862 variables converged at R_1=7.23 % for the observed data and wR_2=18.35 % for all data. The goodness-of-fit was 1.000. The largest peak on the final difference map was 0.576$\bar{e}$/$Å^3$ and the largest hole was -0.852$\bar{e}$/$Å^3$. On the basis of the final model, the calculated density was 1.691 g/cm^3 and F(000), 11016$\bar{e}$.

Overall structure quality considerations:

1. Strong data set, no disorder, R_1 4% maximum. Publishable quality.
2. Good data set, perhaps some minor disorder, $R_1$6% maximum. Publishable quality.
3. **Average data set and/or easily modeled disorder or twinning. Publishable with care.**
4. Weak data and/or major disorder or twinning that is not easily modeled. Publishable in some cases.
5. Very weak data and/or unexplained features of data or model. Not of publishable quality.

A structure with a quality factor of 4 or 5 should not be used for a regulatory document without prior consultation.

Comments:

- Data quality:	good
- Twinning:	merohedral, refined using twin/basf to 7:1 ratio
- Disorder:	substantial disorder of water and iodine ions; accounted for using squeeze (see CIF for details); guest molecule disordered in two orientations in about 1:1 ratio
- H-atoms:	constrained geometry as riding on attached atom (A) Uiso(H)=1.5*U_{iso}(A) for CH_3 and 1.2*U_{iso}(A) for other groups
- Residual density:	near heavy atoms &near disordered groups
- Structure quality:	good & average because of strong disorder and significantly elevated thermal motion of guest
Publishable	Yes with care

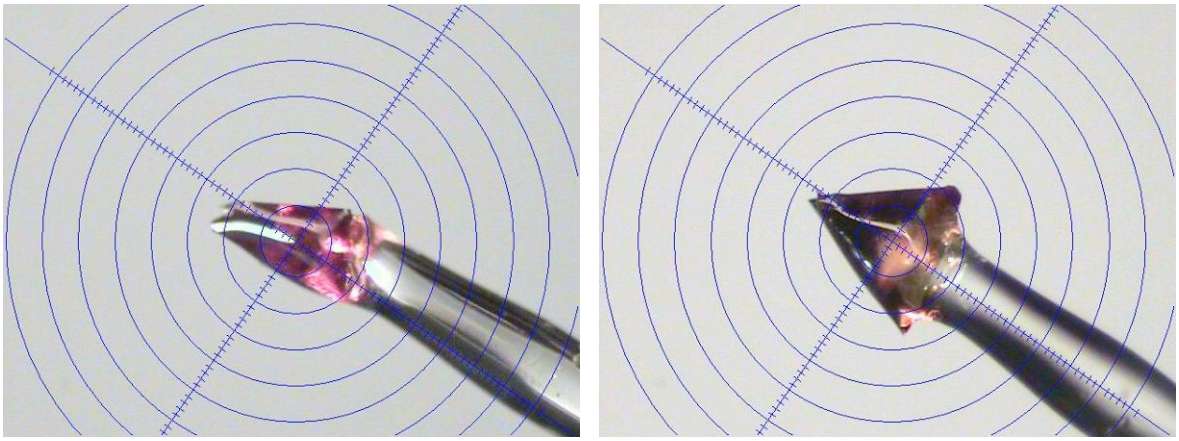

Table S2. Crystal data and structure refinement for UM#1597.

X-ray lab book No.		1597
Crystal ID		Isaacs/Wei-Hao Huang 1,9 @150K
Empirical formula		$C_{52}H_{94}I_2N_{26}O_{28}$
Formula weight		1785.33
Temperature		150(2) K
Wavelength		0.71073 Å
Crystal size		0.39 × 0.35 × 0.195 mm^3
Crystal habit		yellow prism
Crystal system		Cubic
Space group		$P2_13$
Unit cell dimensions		a = 27.6038(2) Å α = 90°
		b = 27.6038(2) Å β = 90°
		c = 27.6038(2) Å γ = 90°
Volume		21033.3(3) $Å^3$
Z		12
Density, ρ_{calc}		1.691 g/cm^3
Absorption coefficient, μ		1.000 mm^{-1}
F(000)		11016ē
Diffractometer		Bruker Smart Apex II CCD area detector
Radiation source		fine-focus sealed tube, MoKα
Detector distance		6.00 cm
Detector resolution		83.33 pixels/mm
Total frames		2035
Frame size		512 pixels
Frame width		0.3°
Exposure per frame		30 sec
Total measurement time		20.1 hours
Data collection method		ω and φ scans
q range for data collection		1.81 to 22.49°
Index ranges		$-29 \le h \le 29$, $-29 \le k \le 27$, $-29 \le l \le 29$
Reflections collected		134638
Independent reflections		9175
Observed reflection, I>2s(I)		8432
Coverage of independent reflections		99.8 %
Variation in check reflections		0 %
Absorption correction		Semi-empirical from equivalents
		SADABS (Sheldrick, 1996)
Max. and min. transmission		0.823 and 0.734
Structure solution technique		direct
Structure solution program		SHELXS-97 (Sheldrick, 1990)
Refinement technique		Full-matrix least-squares on F^2
Refinement program		SHELXL-97 (Sheldrick, 1997)
Function minimized		$\_w(F_o^2 - F_c^2)^2$
Data / restraints / parameters		9175 / 189 / 862
Goodness-of-fit on F^2		1.003
D/s_{max}		0.001
Final R indices:	R_1, I>2s(I)	0.0723
	wR_2, all data	0.1835
	R_{int}	0.0531
	R_{sig}	0.0237
Weighting scheme		$w = 1/[\sigma^2(F_o^2)+(0.09P)^2+87P]$, $P = [\max(F_o^2,0)+2F_o^2]/3$
Absolute structure parameter		0.13(3)
Largest diff. peak and hole		0.576 and -0.852ē /$Å^3$

$R_1 = \Sigma||F_o|-|F_c||/\Sigma|F_o|$, $wR2 = [\Sigma w(F_o^2 - F_c^2)^2/\Sigma w(F_o^2)^2]^{1/2}$

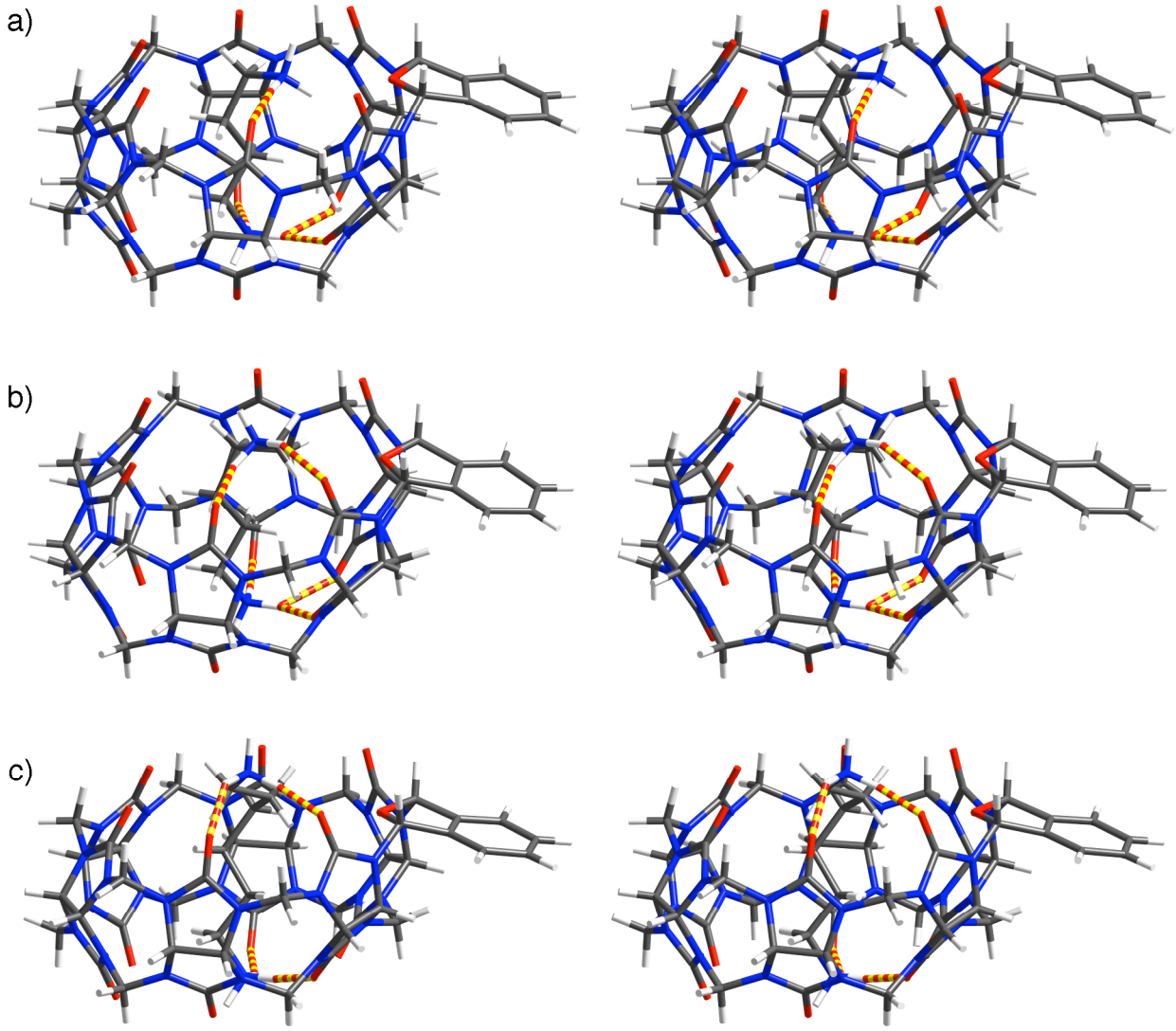

Figure S43. Cross-eyed stereoviews of MMFF minimized geometries of: a) **2•3a**, b) **2•3b**, c) **2•3c**. Color code: C, grey; H, white; N, blue; O, red; H-bonds, red-yellow striped.

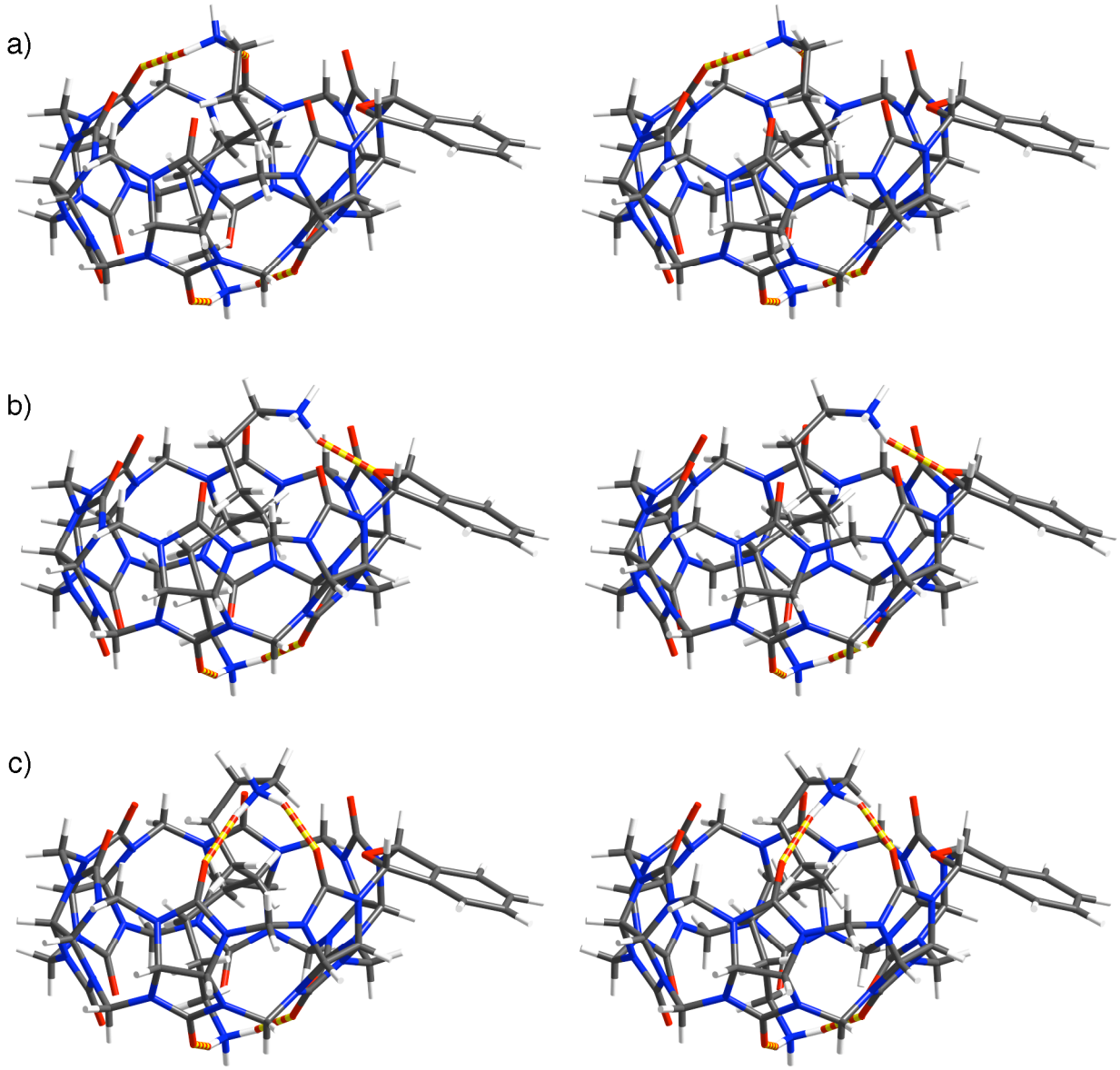

Figure S44. Cross-eyed stereoviews of MMFF minimized geometries of: a) **2•3d**, b) **2•3e**, c) **2•3f**. Color code: C, grey; H, white; N, blue; O, red; H-bonds, red-yellow striped.

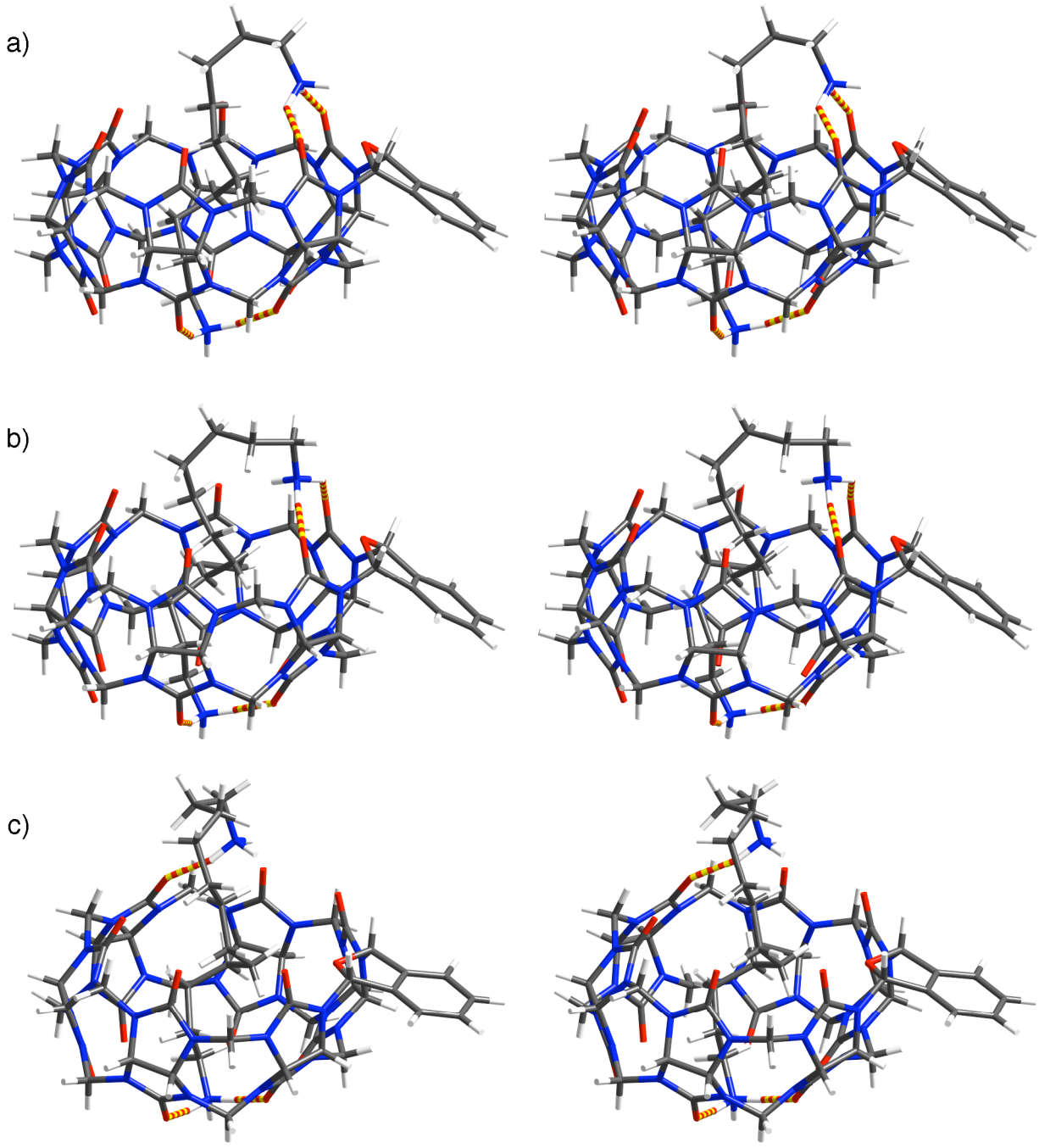

Figure S45. Cross-eyed stereoviews of MMFF minimized geometries of: a) **2•3g**, b) **2•3h**, c) **2•3i**. Color code: C, grey; H, white; N, blue; O, red; H-bonds, red-yellow striped.

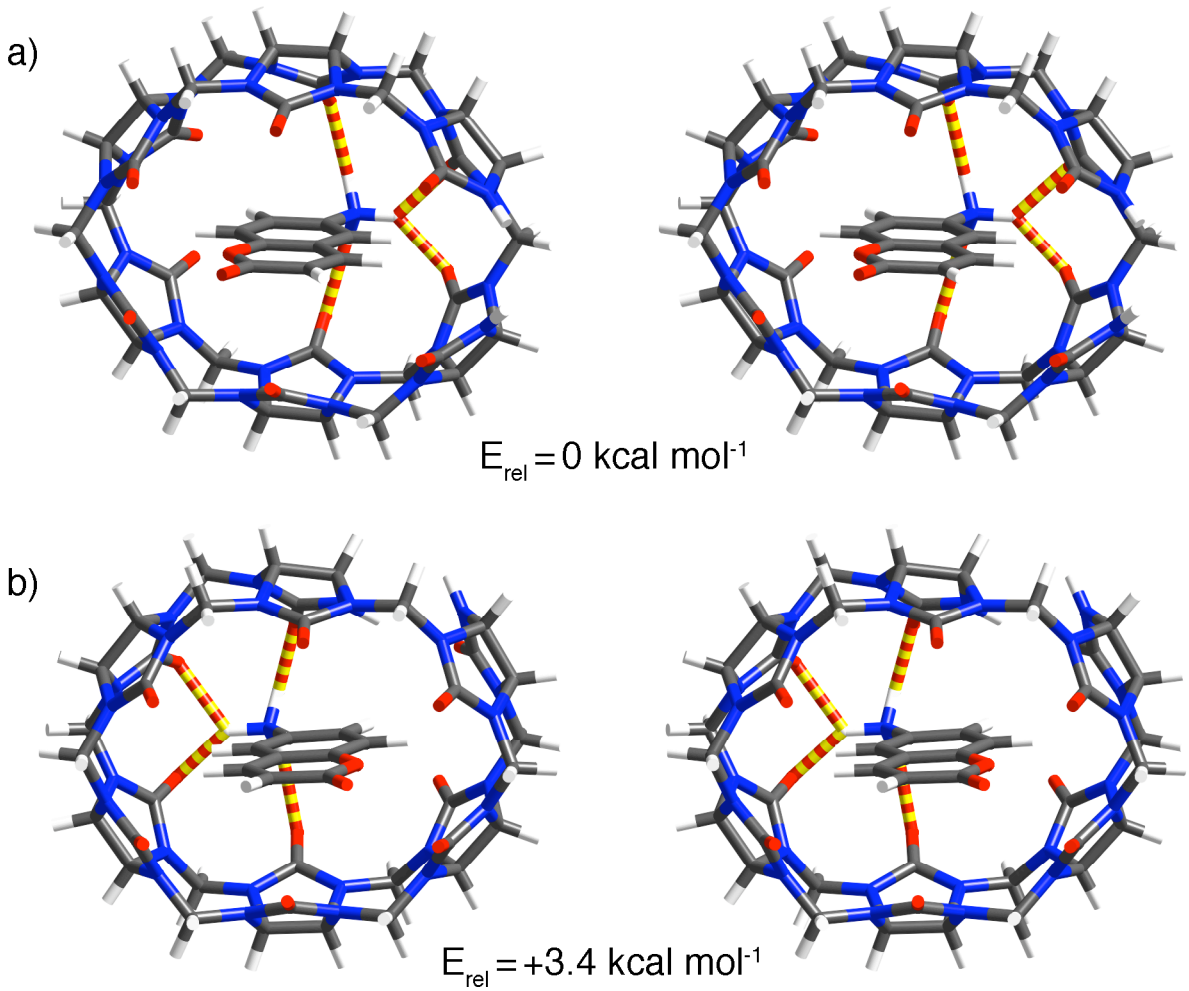

Figure S46. Cross-eyed stereoviews of MMFF minimized geometries and heats of formation for: a) bottom-*ns*-CB[6]•**9**, and b) top-*ns*-CB[6]•**9**. Color code: C, grey; H, white; N, blue; O, red; H-bonds, red-yellow striped.

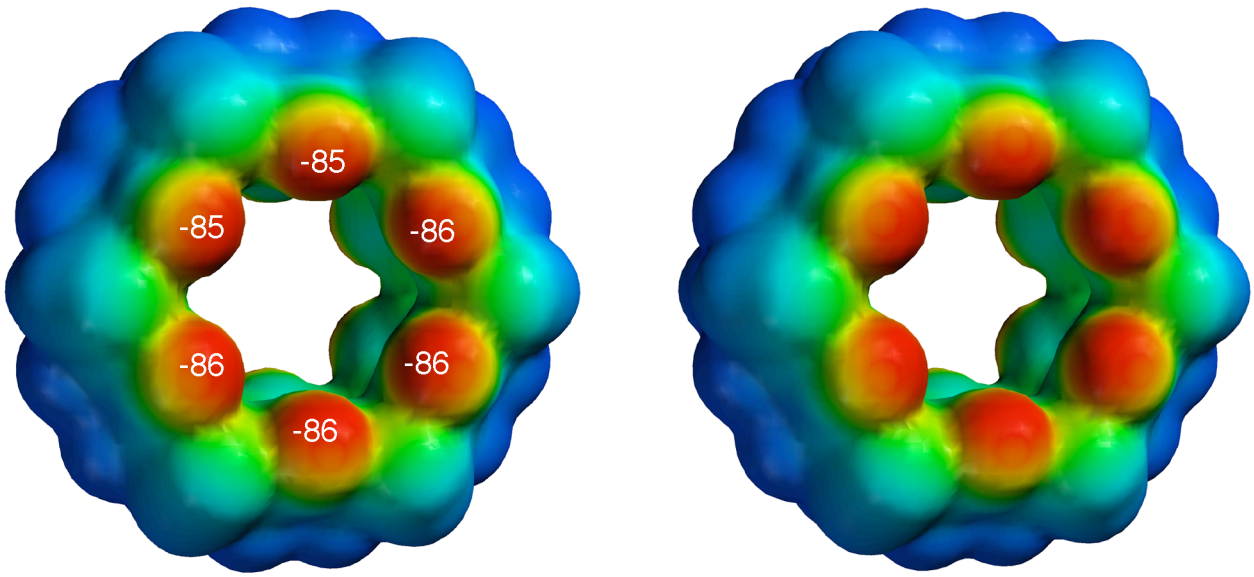

Figure S47. Stereoscopic representation of the electrostatic surface potential (PM3) plot for CB[6]. The red to blue color range spans –85 to +35 kcal mol^{-1}.

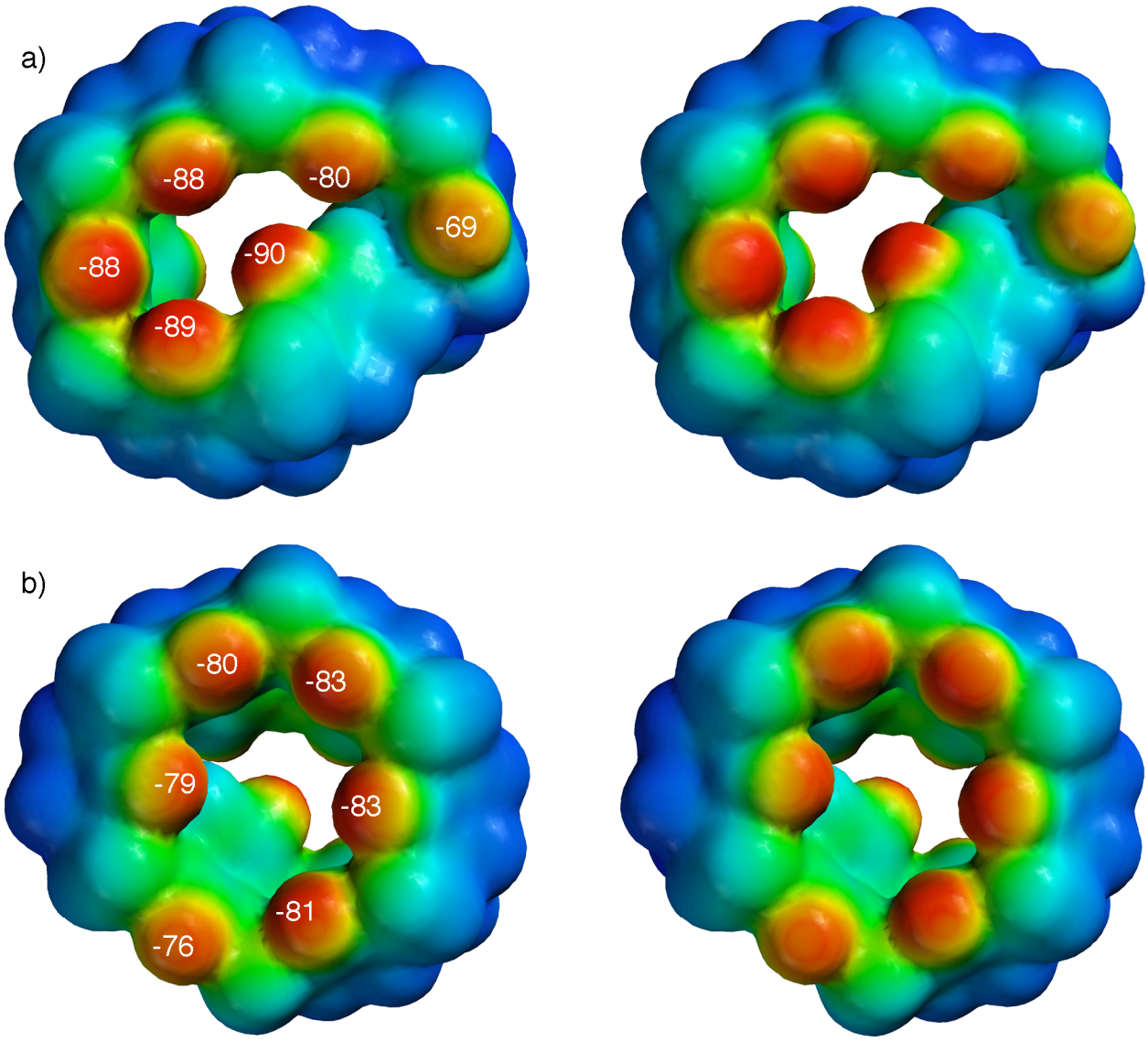

Figure S48. Stereoscopic representations of the electrostatic surface potential (PM3) plot for the MMFF minimized geometry of *ns*-CB[6]: a) top view, and b) bottom view. The red to blue color range spans –85 to +35 kcal mol^{-1}.

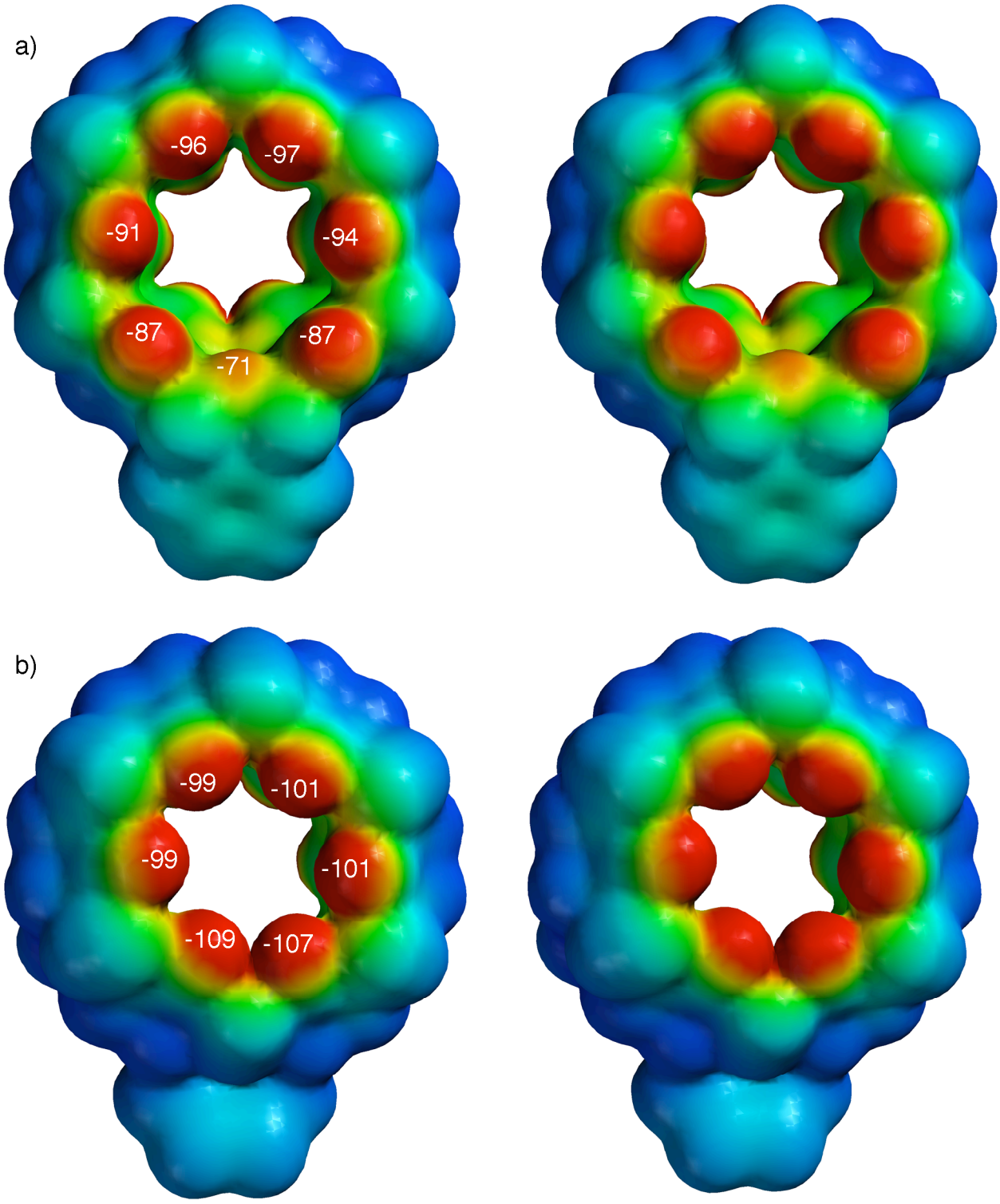

Figure S49. Stereoscopic representation of the electrostatic surface potential (PM3) plot for **2**: a) top view, and b) bottom view. The red to blue color range spans –85 to +35 kcal mol^{-1}.